(TOF) Neutron Imaging

G.Salvato – CNR IPCF

Messina

***What** is Neutron Imaging ?*

Guess what…

A technique to *obtain images of the **inner parts** (radiography) of an object using a **neutron beam** to illuminate it.*

Results are **similar** to the ones obtained using X-rays…

X-Rays vs Neutron Imaging

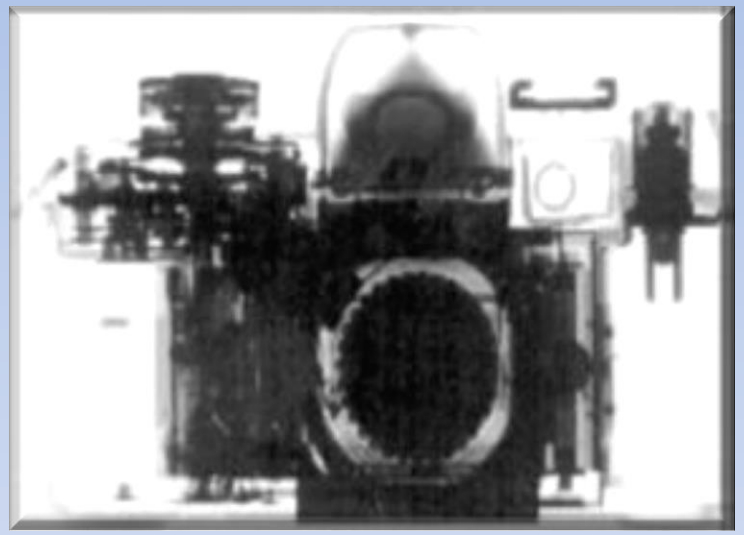

X-Rays[2]

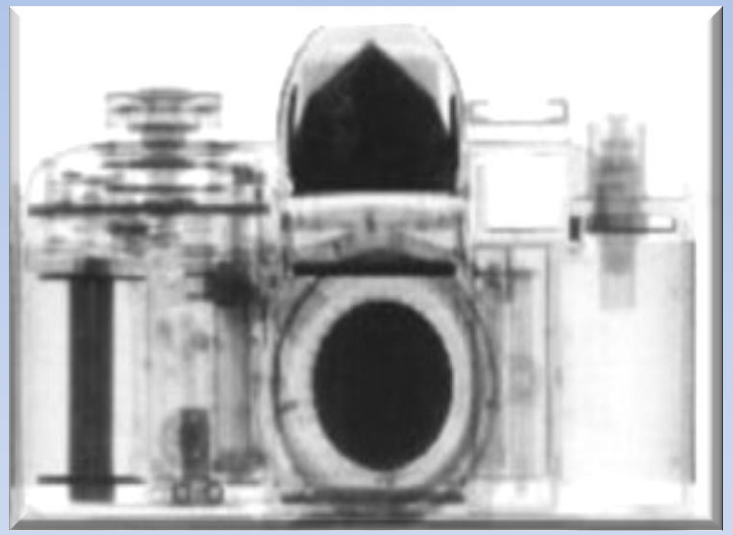

Neutrons [2]

[2] Lehmann, et al. 2000 - http://neutra.web.psi.ch/What/index.html

Results are ***similar but not equal*** to the ones obtained using X-rays… because of the different ***mass attenuation coefficients.***

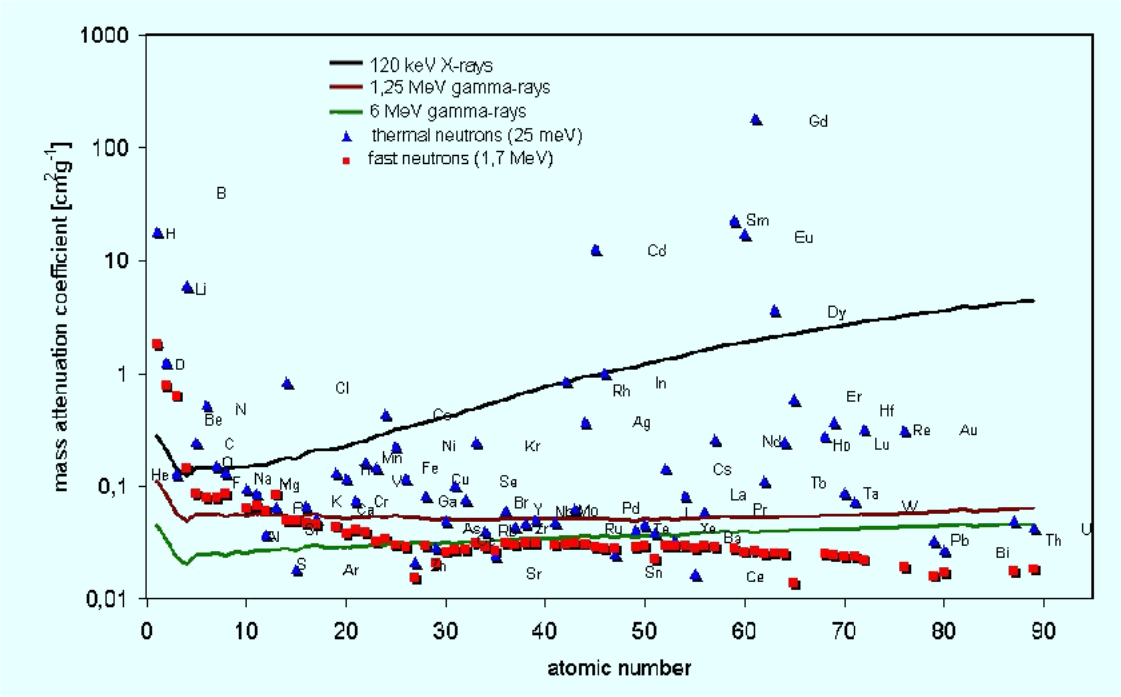

B.Schillinger http://www.frm2.tum.de/fileadmin/stuff/events/VDI_WExpertenforum/talks/TUM-Industrietag_Schillinger.pdf

Why use Neutrons for Imaging ?

The transmission of **X-rays** through the matter is described by the ***Lambert-Beer law***

$$I = I_0 e^{-\left[\left(\frac{\mu}{\rho}\right)\rho\, d\right]}$$

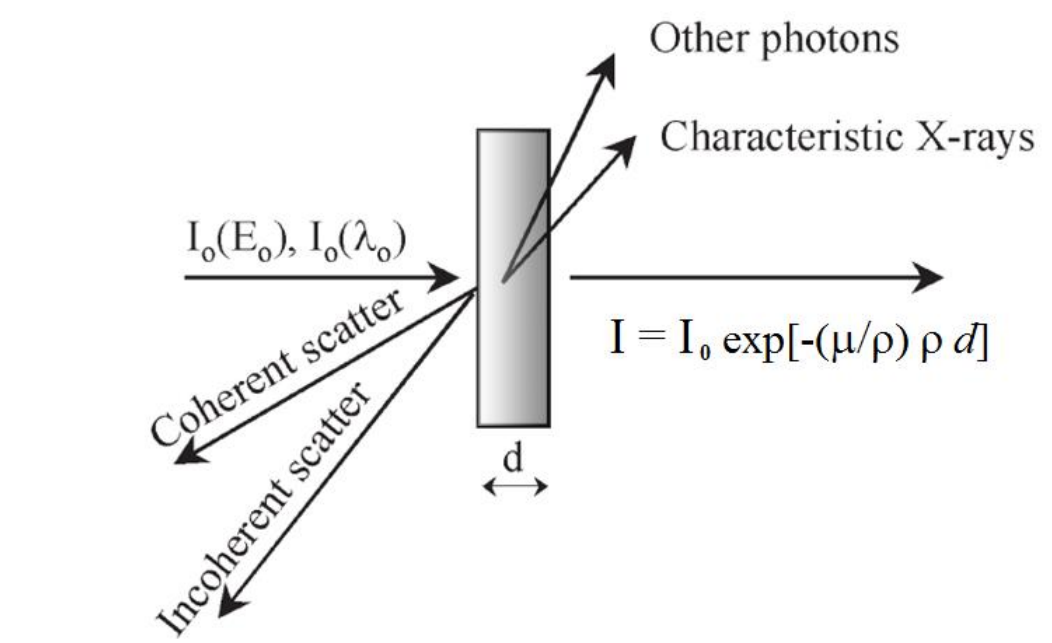

μ/ρ : *mass attenuation coefficient* [$cm^2 g^{-1}$].

ρ : *material density* [$g\ cm^{-3}$].

The transmitted intensity of **X-rays** through the matter is tied to the ***interaction between X photons and the electronic shells*** *of the atoms.*

The attenuation grows, almost linearly, with the atomic number

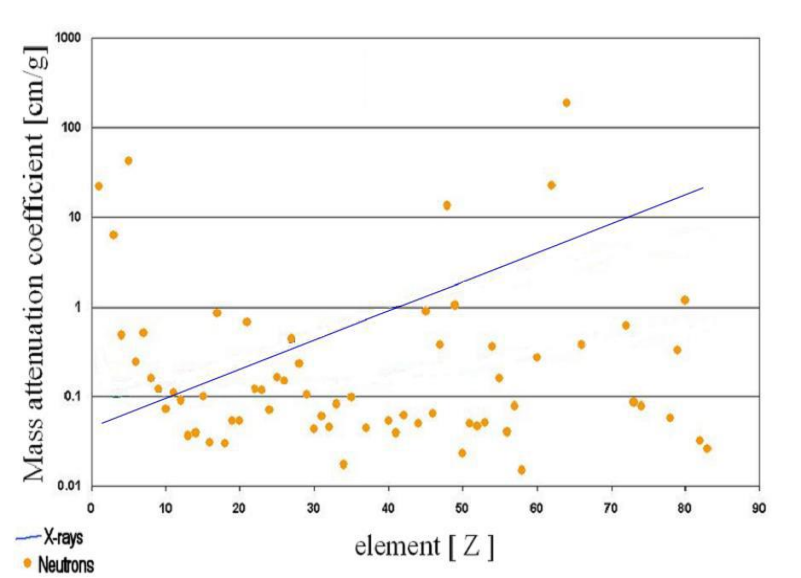

R.Pynn – Neutron Scattering: A Primer - Los Alamos Science (1992)

The attenuation is high for high-Z materials and low for low-Z ones.

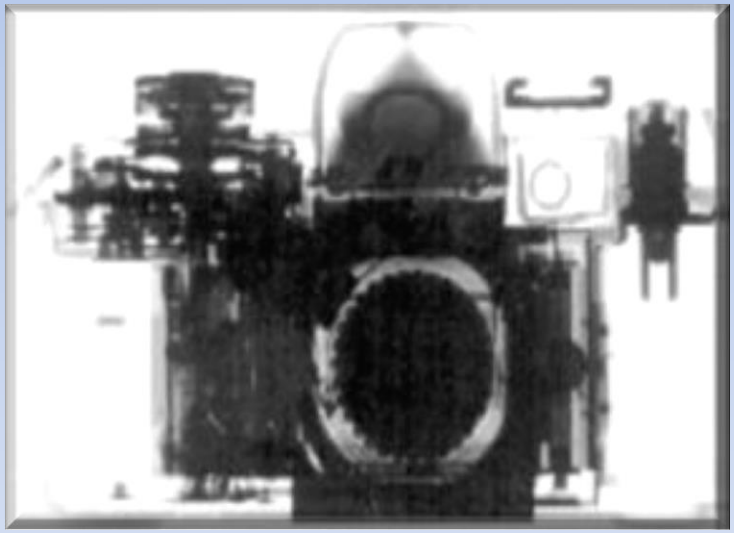

X-Ray Image

The transmission of a **neutron beam** through the matter is described too by the ***Lambert-Beer law:***

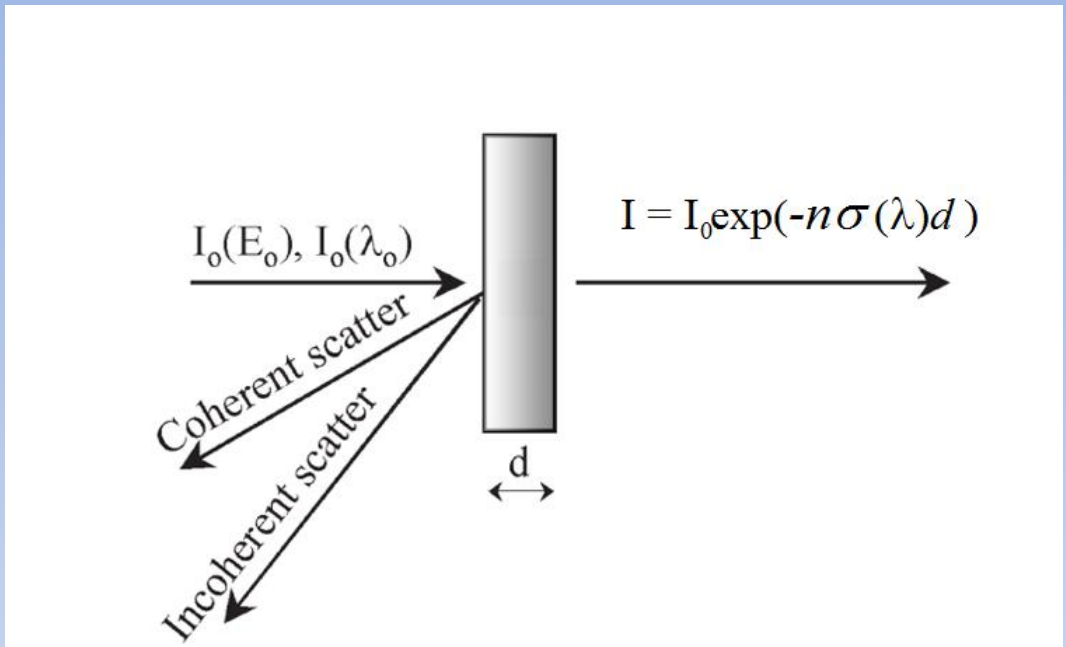

$$I(\lambda) = I_0(\lambda)e^{-n\sigma(\lambda)d}$$

n : *scattering center number.*

$\sigma(\lambda)$: *total cross-section per scattering center.*

Because of the charge neutrality of neutrons the transmitted intensity is **NOT** tied to the Z number

The attenuation is randomly distributed among different materials allowing different contrast even between materials with similar Z numbers

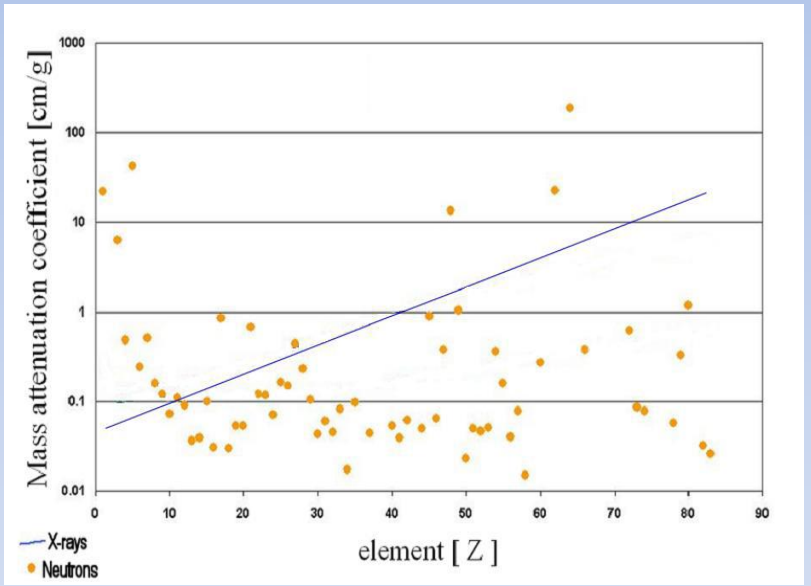

Neutrons are able to ***distinguish between different isotopes*** of the same substance.

Isotope	absorption cross section for 1.8Å neutrons	Isotope	absorption cross section for 1.8Å neutrons
^{1}H	0.3326	^{2}H	0.000519
^{6}Li	940	^{7}Li	0.0454
^{3}He	5333	^{4}He	0 .000…
^{10}B	3835	^{11}B	0.0055
^{157}Gd	259000	^{158}Gd	2.2

***Why** to use Neutrons for Imaging ?*

Light atoms (*H*, *Li*, *B*), almost transparent to X-rays, give a good contrast when imaged with neutrons while heavy atoms are not opaque.

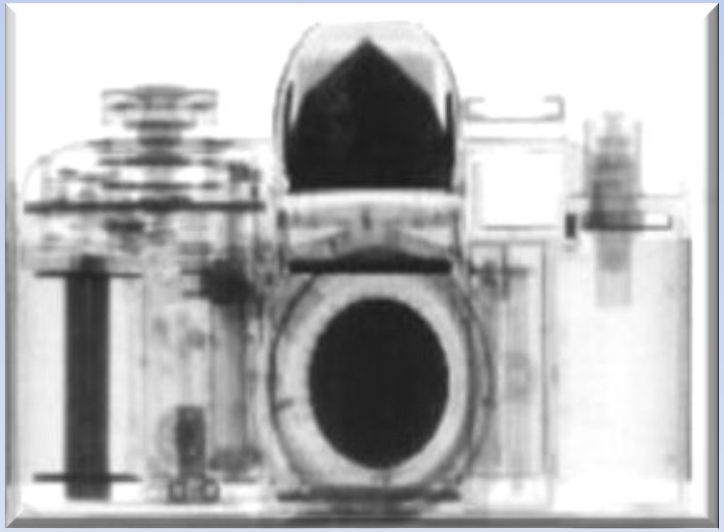

Neutron Image

Heavy metals (*Pb*, *Fe*), almost opaque to X-rays, can be imaged with good contrast with neutrons.

Lead's cannonball (906g) from the ***Bosworth Field (1485)*** battle.
(*Wars of the Roses)*

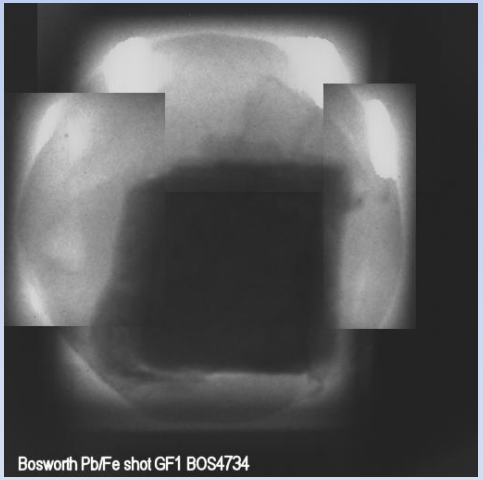

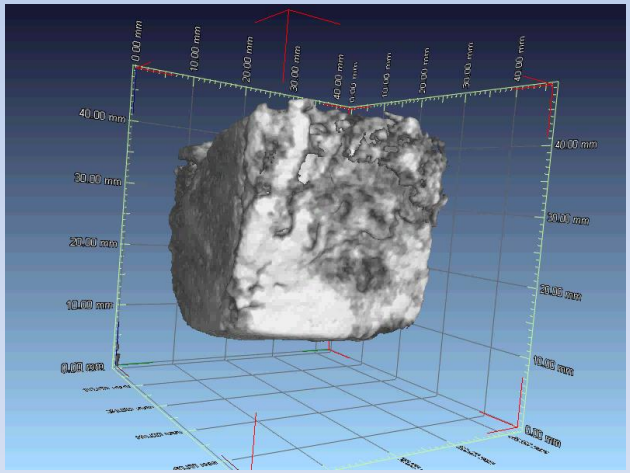

E.Godfrey, W.Kockelmann, G.Salvato, D.Tresoldi "*Non-invasive Neutron Techniques: implications for analysis of battlefield artefacts" (2010)*

***How** Neutron Imaging is done ?*

Neutron Source

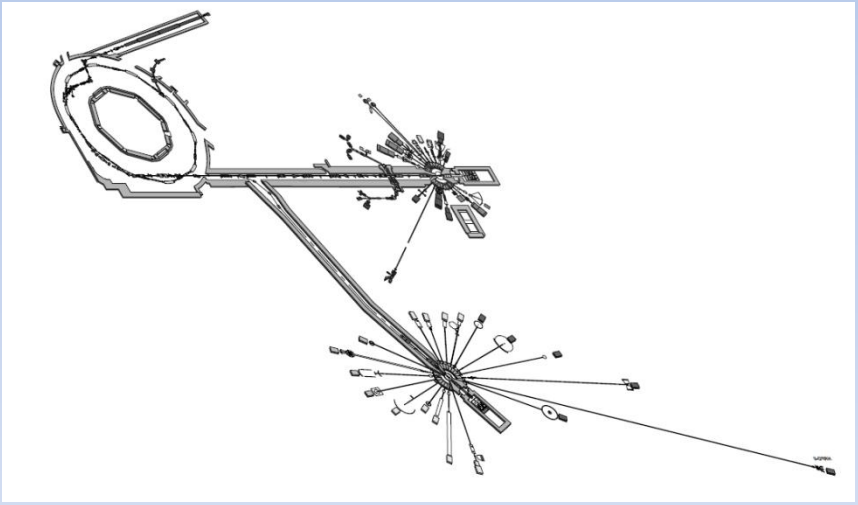

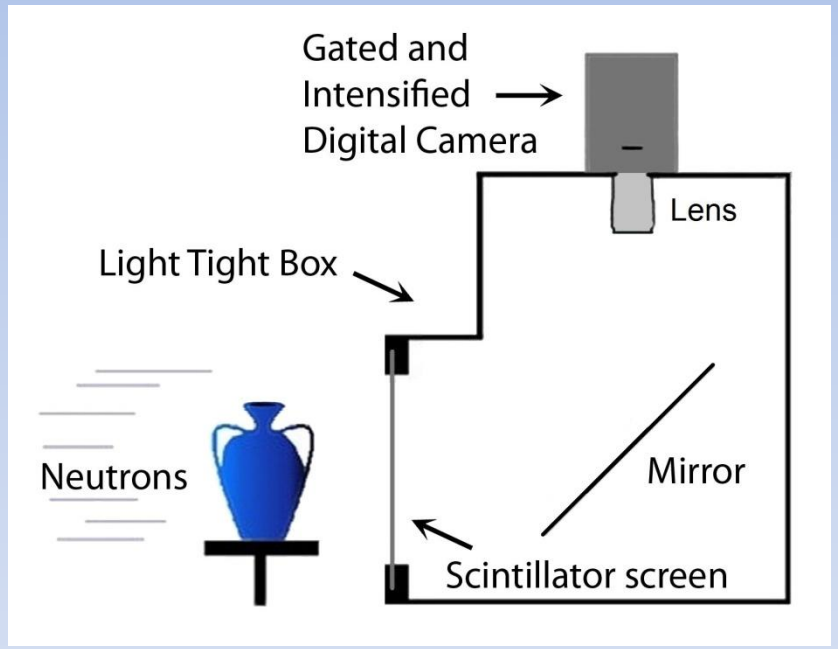

Detector System

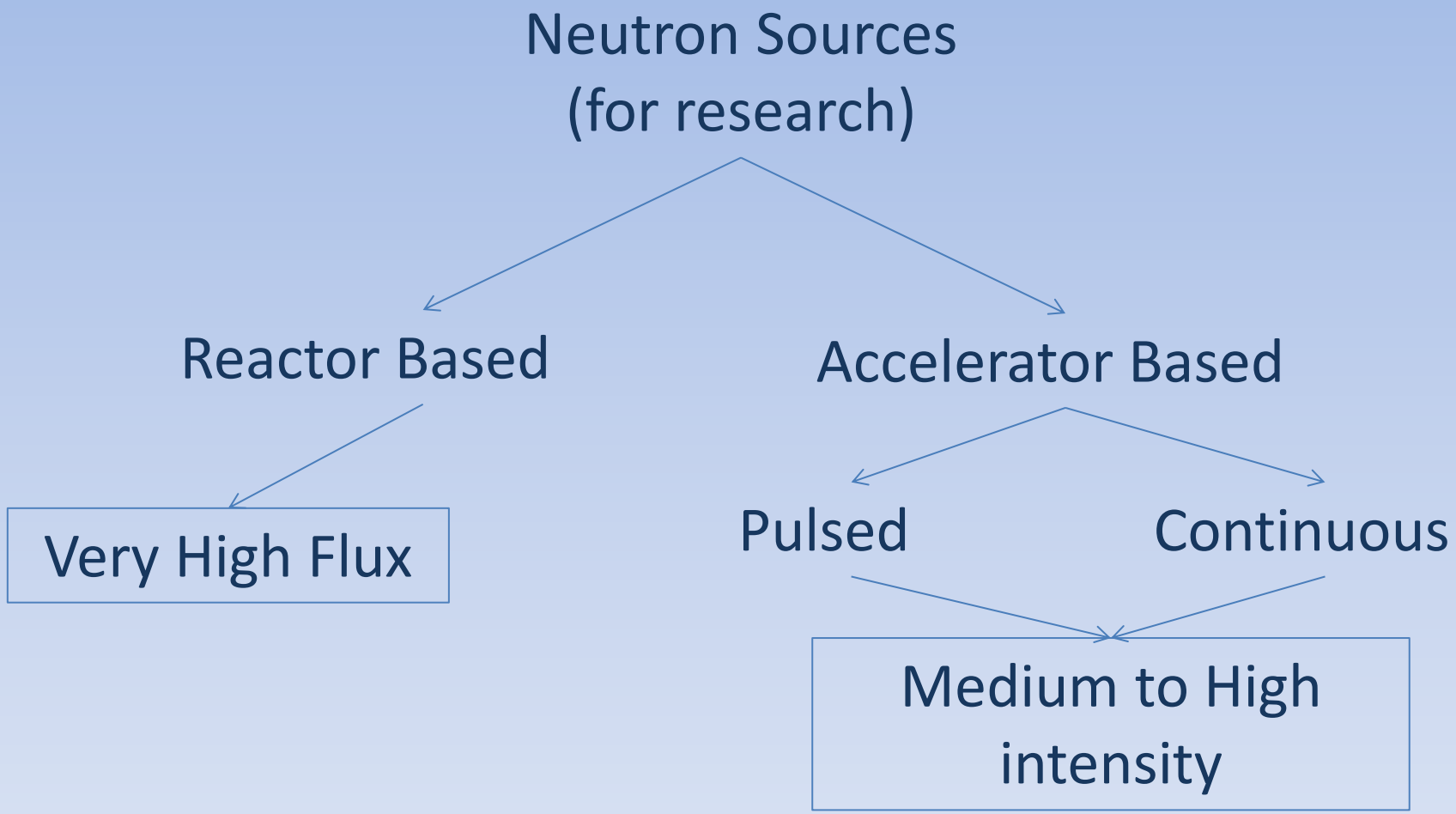
Neutron Sources
(for research)
Reactor Based
Accelerator Based
Very High Flux
Pulsed
Continuous
Medium to High
intensity

STATUS OF NEUTRON IMAGING INSTALLATIONS AT THE NEW PULSED SPALLATION SOURCES [1]

Facility	Status	neutron imaging project
ISIS-TS2 (Rutherford Lab, UK)	under construction	IMAT
SNS (Oak Ridge, USA)	In operation since 2006	VENUS
J-PARC (Tokai, Japan)	in test operation since 2008	considered
ESS (Lund, Sweden)	Under consideration	probable

[1] E.H. Lehmann, A. Kaestner AP/IE (2006)

How *Neutron Imaging is done ?*

Due to their charge neutrality, ***neutrons are difficult to detect***.

Instead, ***we are good in detecting charged particles***.

A nuclear reaction is needed to convert incoming neutrons into charged particles.

Depending on the employed image sensor further conversions can be necessary.

As an example, if the image formation sensor is a ***digital camera*** (or an imaging plate) the charged particles must be converted into ***photons***.

Other type of sensors are able to produce images directly from the charged particles.

Timepix/Medipix *(discussed in the following)* based sensor are an example of such devices.

A number of different reactions can be used to convert neutrons into charged particles.

Main reactions employed : [1]

$n + {}^{3}He \rightarrow p\,(+578KeV) + {}^{3}H(+193KeV)$ $\quad \sigma = 28000$ b

$n + {}^{6}Li \rightarrow {}^{4}He(+2.05MeV) + {}^{3}H(+2.73MeV)$ $\quad \sigma = 520$ b

$n + {}^{10}B \rightarrow {}^{7}Li^{*}(+0.83MeV) + {}^{4}He(+1.47MeV)$

$\downarrow$

$\gamma(+0.48MeV)\ (93\%)$

$\rightarrow {}^{7}Li(+1.0MeV) + {}^{4}He(+1.8MeV)\ (7\%)$ $\quad \sigma = 2100$ b

σ @ 1Å

[1] C.W.E. van Eijk Nucl. Instr. And Meth. A **477** 383 (2002)

Main reactions employed : [1]

$$n + {}^{157}Gd \rightarrow {}^{158}Gd + \gamma + \text{conversion electrons}$$

(29-182KeV)

σ = 70000 b

$$n + {}^{155}Gd \rightarrow {}^{156}Gd + \gamma + \text{conversion electrons}$$

(39-199KeV)

σ = 17000 b

σ @ 1Å

[1] C.W.E. van Eijk Nucl. Instr. And Meth. A **477** 383 (2002)

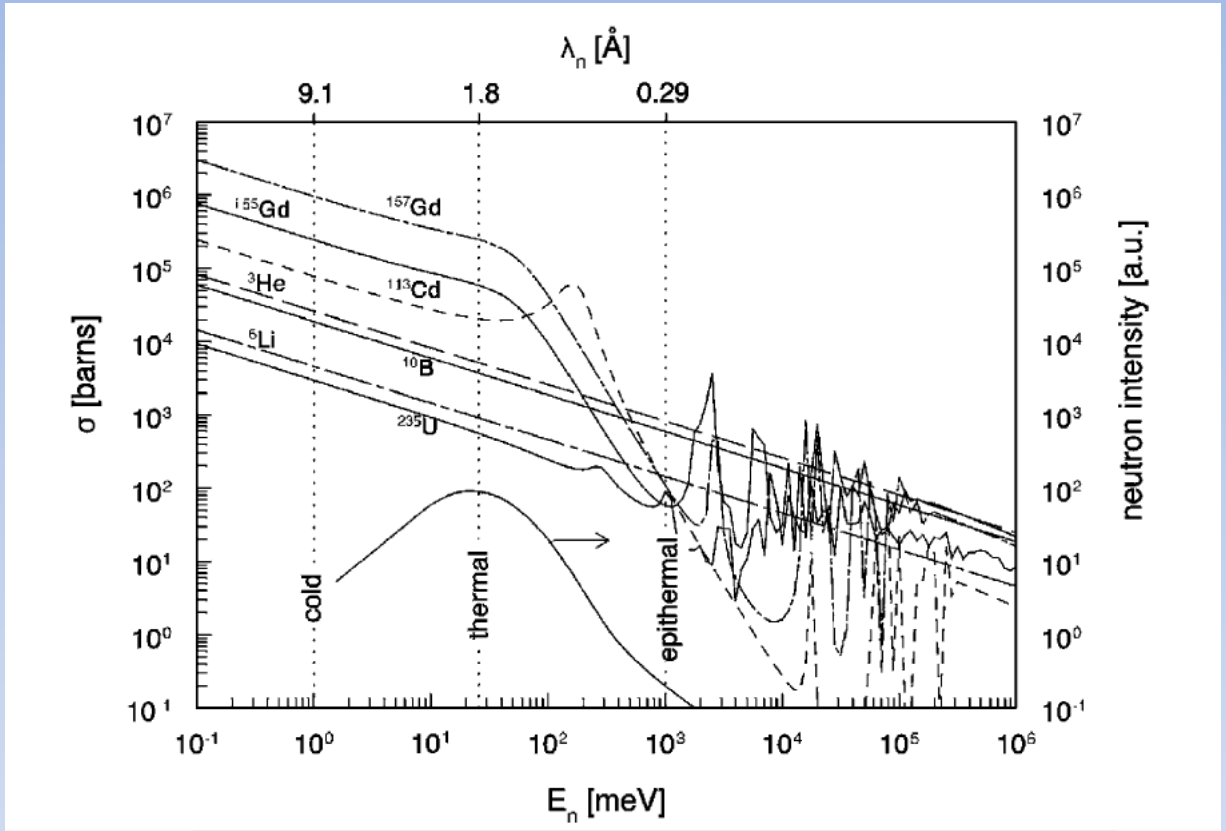

Neutron capture cross-sections of some isotopes important for neutron detectors as a function of neutron energy. The lowest curve shows a typical moderated-neutron spectrum of a nuclear reactor (right y-axis) [1].

[1] C.W.E. van Eijk Nucl. Instr. And Meth. A **477** 383 (2002)

Camera based Imaging Systems

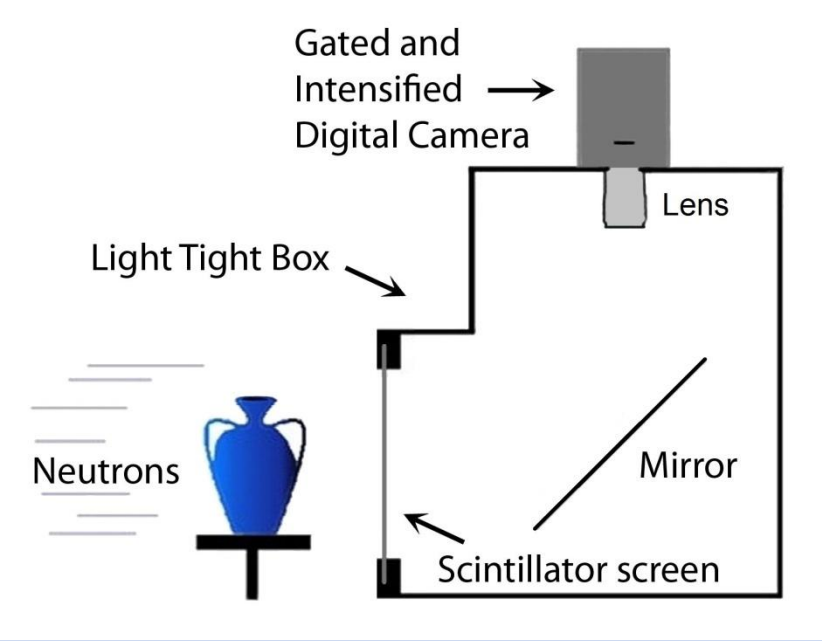

A general setup for the digital camera based neutron imaging system is depicted on the side.

A ***scintillator screen*** converts the incoming neutrons into photons.

The most used scintillator screens are made by a mix of finely grounded ^{6}***LiF*** and ***ZnS:Ag*** *or* ***ZnS:Cu*** powders.

The ^{6}***LiF*** and ***ZnS:Ag*** *or* ***ZnS:Cu*** powders are mixed with an organic binder and deposited on a thin ***Al*** foil.

The ***Al*** foil is almost transparent to neutrons but it stops the light from the outside.

When a ^{6}***Li*** atom interacts with a neutron it emits a *Triton* and an α particle. ***The respective ranges are about 30μm and 5μm*** [1].

[1] T.K. McKnight Master Thesis - Dep. Of Physics and Astronomy – Brigham Young University (2005)

The alpha particles (mainly) interact with the ***ZnS*** phosphor producing about 160.000 photons per neutron [1].

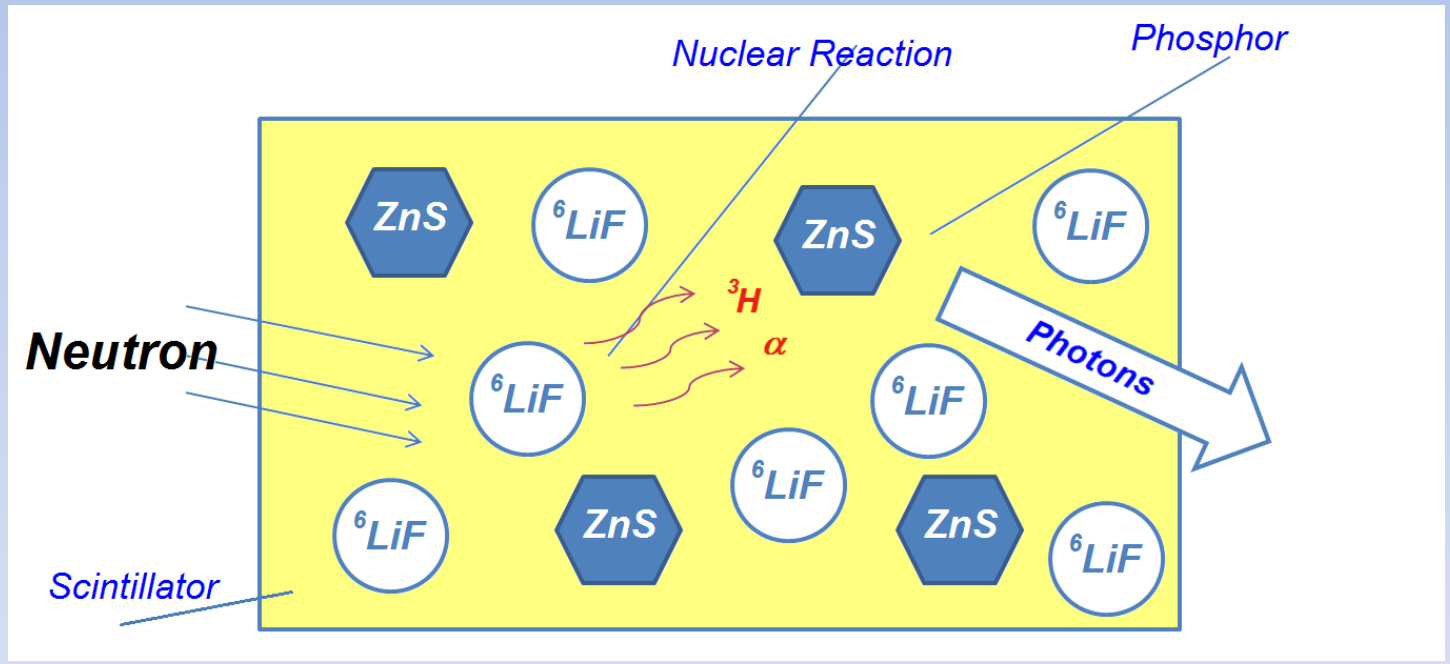

[1] C.W.E. van Eijk Nucl. Instr. And Meth. A **477** 383 (2002)

The ^{6}***LiF/ZnS:Ag*** scintillators produce a blue light (λ~450nm) while the ^{6}***LiF/ZnS:Cu*** *one*s emit in the green region at a wavelength of about 540nm.

The efficiency of the ^{6}***LiF/ZnS*** scintillators grows with their thickness ***BUT*** … since the material ***is opaque at its radiation*** the thickness cannot be greater than 0.4 ~ 0.5mm.

Moreover the ***spatial resolution*** that can be reached with these scintillators decreases as their thickness increases.

$^{6}LiF/ZnS:Ag$ scintillator

S. Baechler et al. Nucl. Instr. and Meth. A **491** 481-491 (2002)

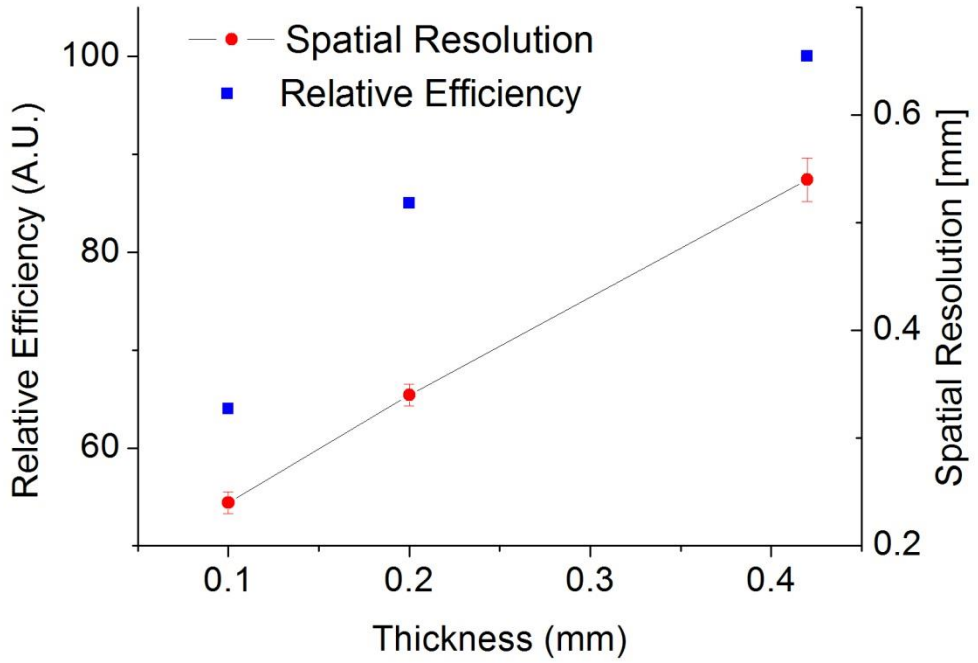

The ultimate limit to the spatial resolution is given by the range of the particles generated by a neutron capture event.

Scintillator spatial resolution

Slanted Edge Method

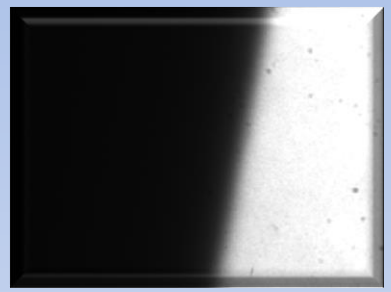

Line Spread Function

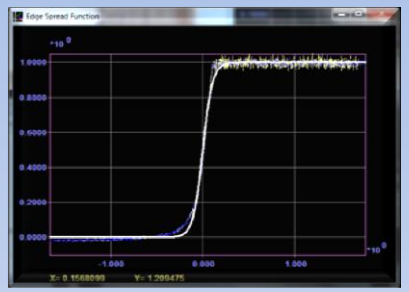

Point Spread Function

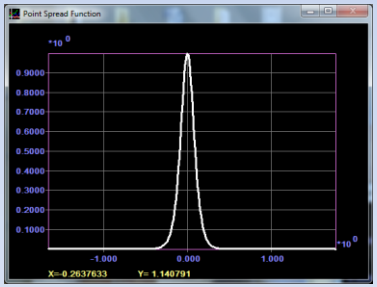

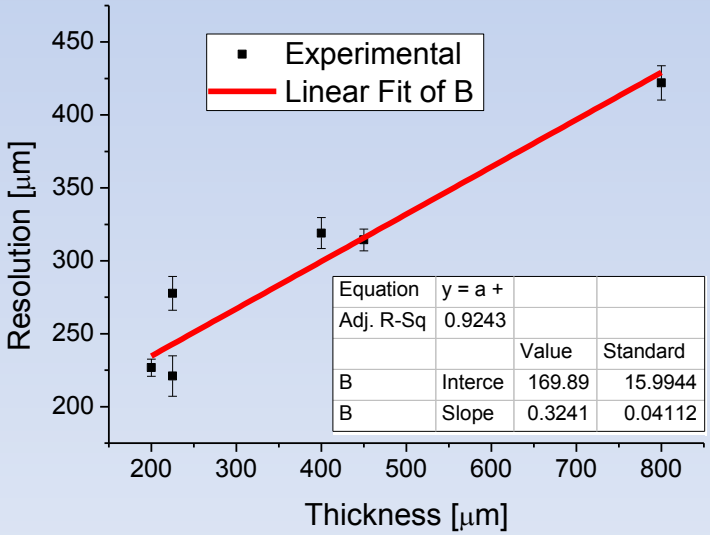

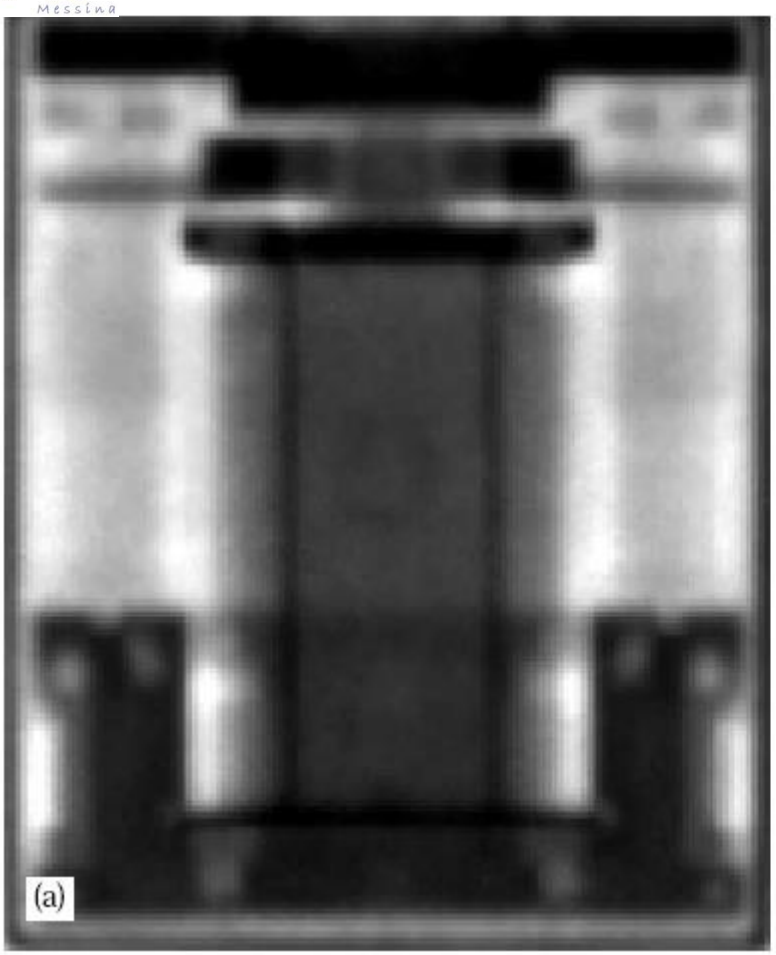

(a) 0.40-mm-thick converter

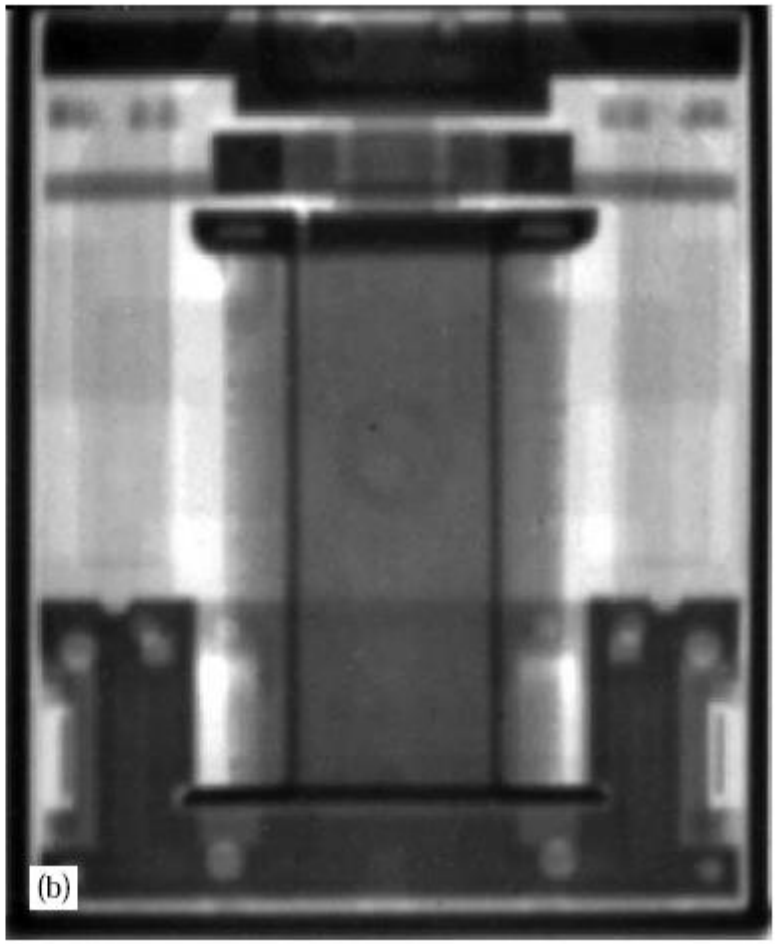

(b) 0.10-mm-thick converter.

S. Baechler et al. Nucl. Instr. and Meth. A **491** 481-491 (2002)

The spatial resolution of a neutron imaging system is tied to many aspects of the experimental setup and not only to the scintillator characteristics.

Among them there are the ***number of pixels*** of the image sensor, the ***field of view dimensions*** and the employed ***optics***.

Moreover, ***the neutron source cannot be considered as a point-like one***. It has a cross-sectional dimension that must be taken into account.

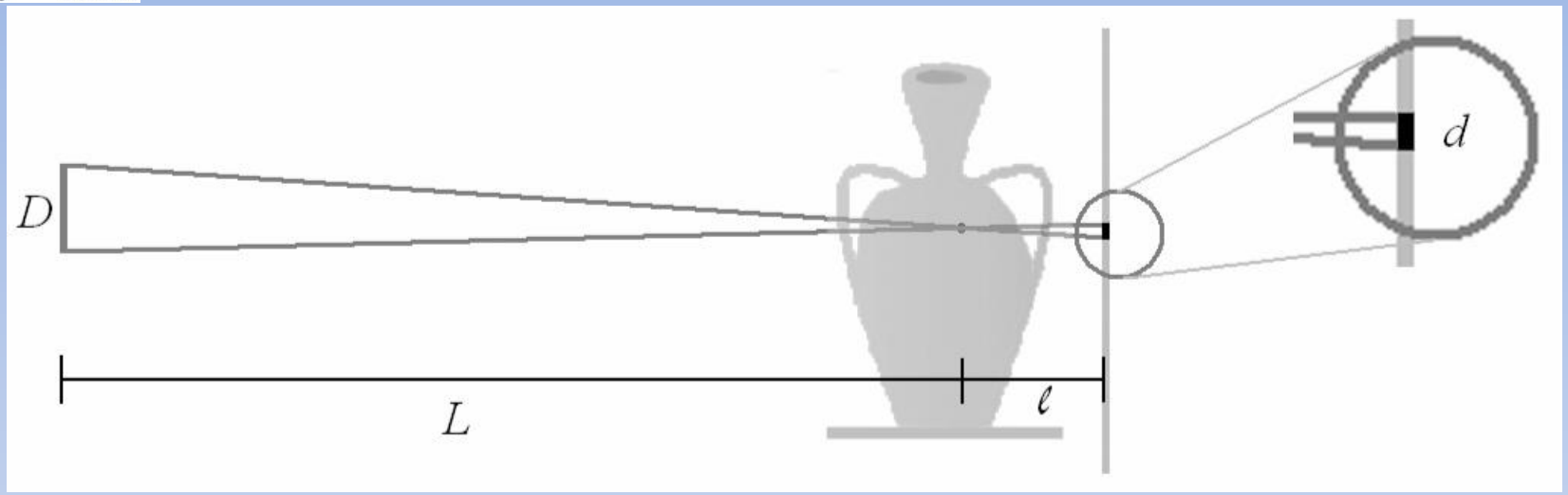

$$d = \ell \frac{D}{L} = \frac{\ell}{L/D}$$

D = neutron source dimension
L = source-sample distance
ℓ = source-scintillator distance

Beam collimation values (***L/D***) greater than 1000 could be found in dedicated neutron imaging beamlines

***What** is Time of flight (TOF) Neutron Imaging ?*

In ***pulsed spallation*** neutron sources, a linear accelerator produces bunches of energetic protons, (~800MeV at ISIS) that are periodically made to collide with a heavy metal ***target***.

For each hit between a proton and a target atom, a number of neutrons (10 - 25) are produced.

Their energy spectrum is peaked toward high energy values.

The neutron energy spectrum is inadequate for the material structure investigations and must be reduced into a wavelength range of 1-10Å

To reduce the neutron energies, they are sent to a ***"moderator"*** that slows the incoming neutron beam.

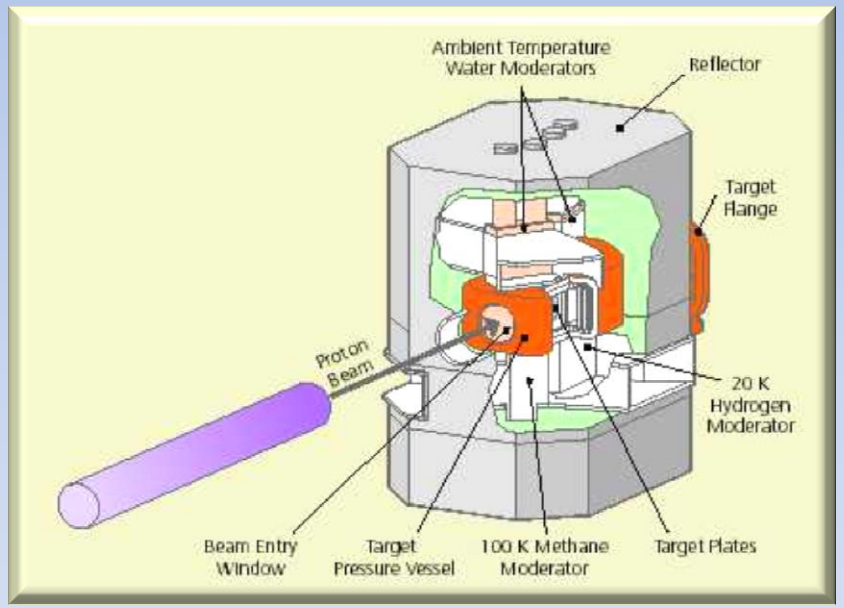

D.Findlay "Introduction to ISIS accelerator and target" (2006)

After the interaction with the moderator nuclei, the neutrons leave the moderator with energies in the wanted energy range (nearly following a Maxwell-Boltzmann distribution).

Because of the different energies with which they leave the moderator, neutrons with wavelength λ arrive at the detector with a TOF *t* given *by:*

$$t = (m L / h) \lambda.$$

The two images below are the measured spectrum of the beamline ROTAX (ISIS - UK) in ***wavelenght*** (left) and ***TOF*** (right).

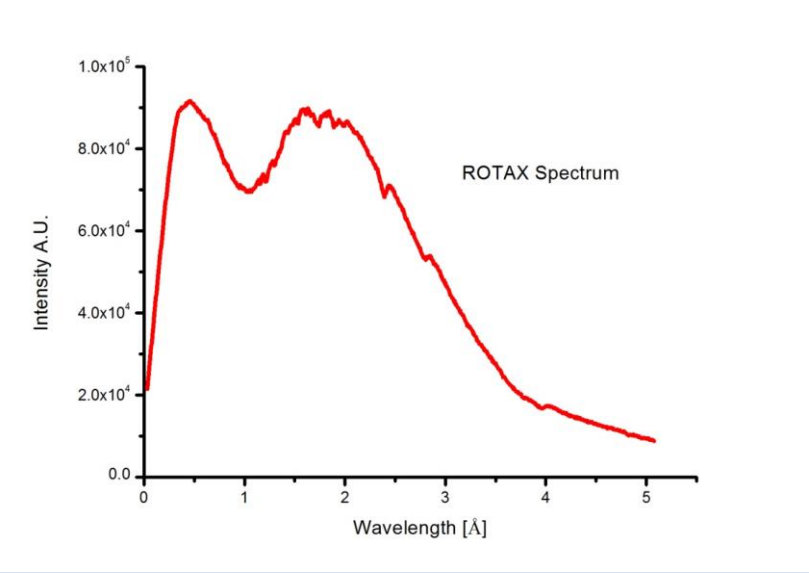

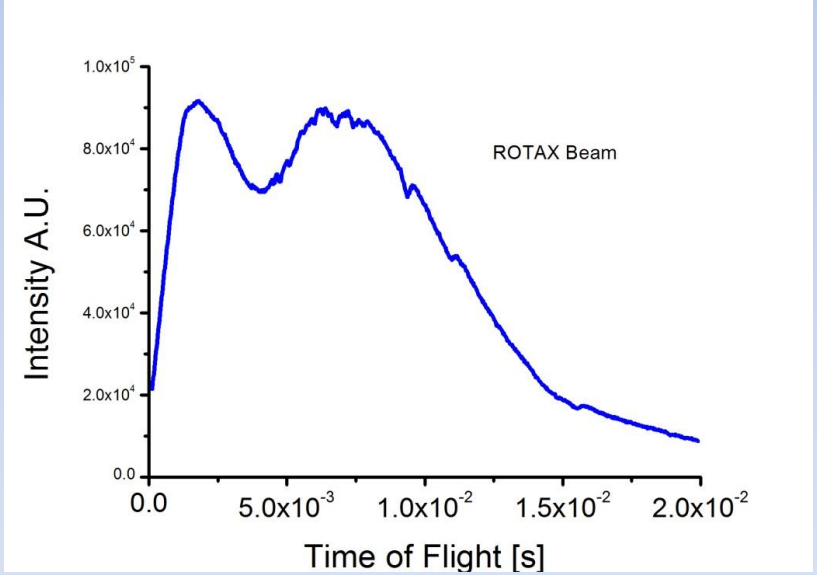

By selecting neutrons in a well determined time relationship with the spallation pulse, we obtain a selection of neutron energies.

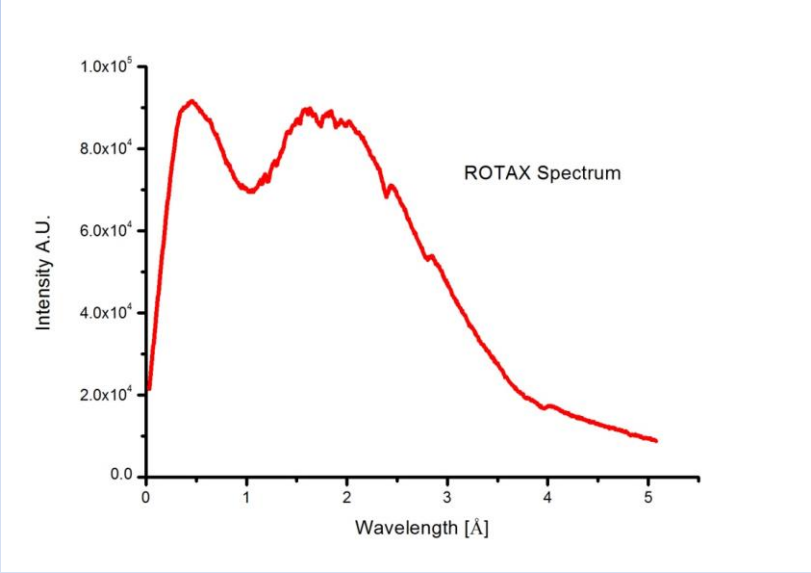

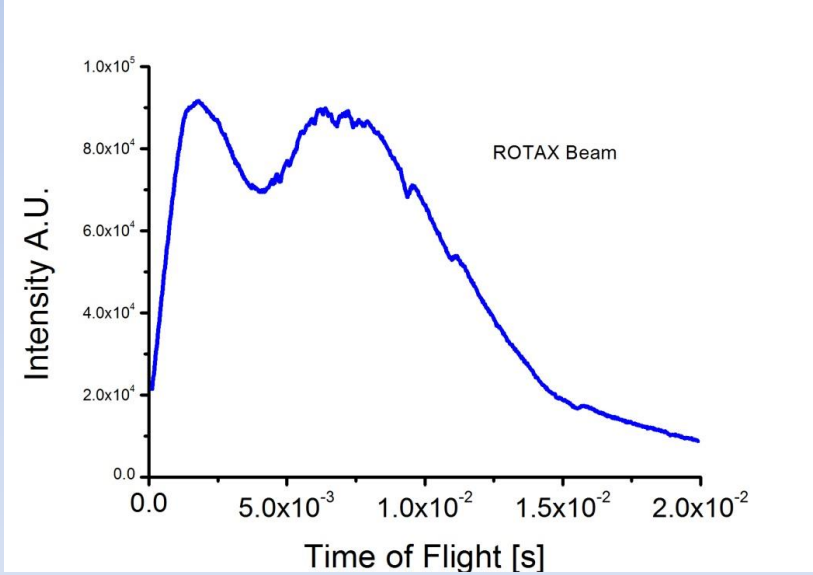

In general, to determine the crystal structure of a polycrystalline sample by ***neutron diffraction***, a wavelength-dependent intensity spectrum is recorded under some angle to the direction of the incident neutron beam.

At certain wavelengths strong intensity maxima are detected: the so-called ***Bragg peaks***.

$$n \cdot \lambda = 2 \cdot d \cdot \sin\theta$$

d is the interplanar distance

2θ is the scattering angle

$n = 1, 2, \ldots$

Bragg's Law

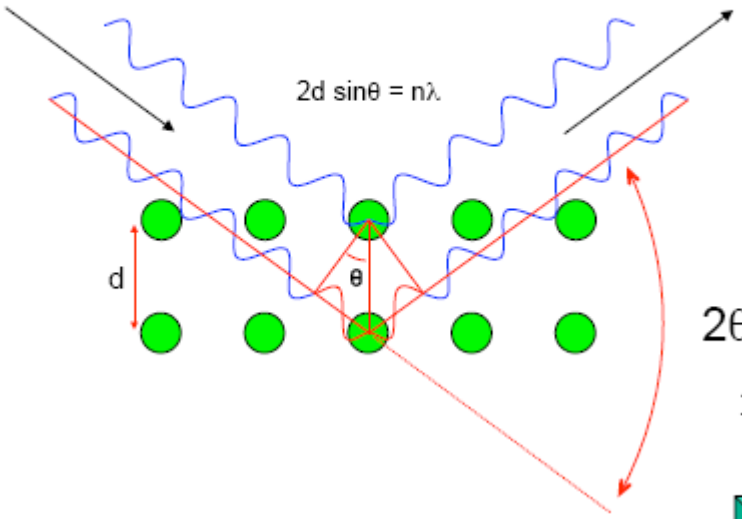

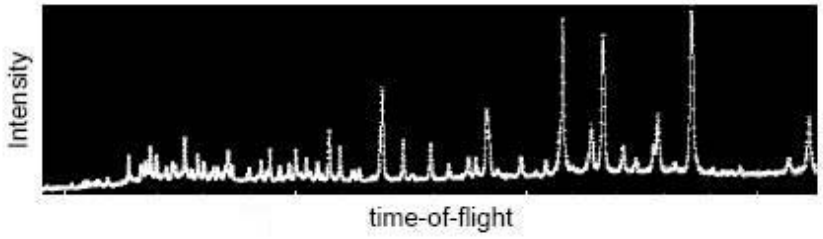

2θ

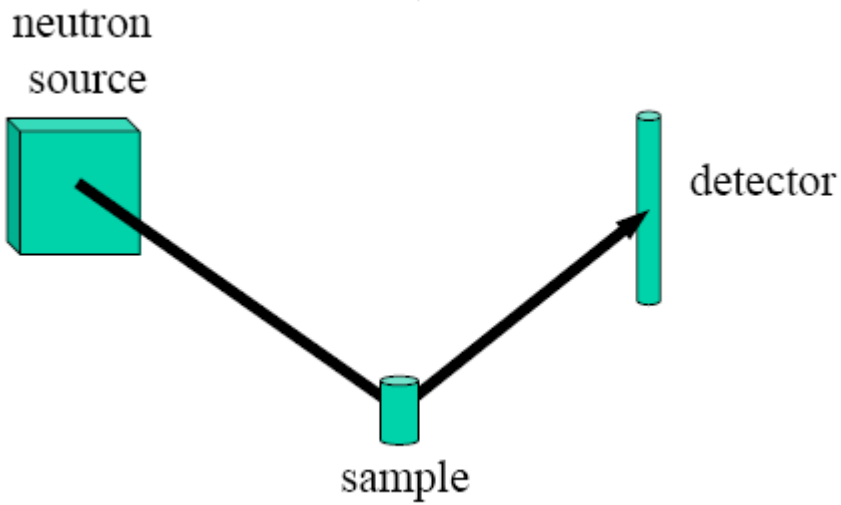

$$n \cdot \lambda = 2 \cdot d \cdot \sin\theta_{fixed}$$

R.Smith "Powder Diffraction" (2009)

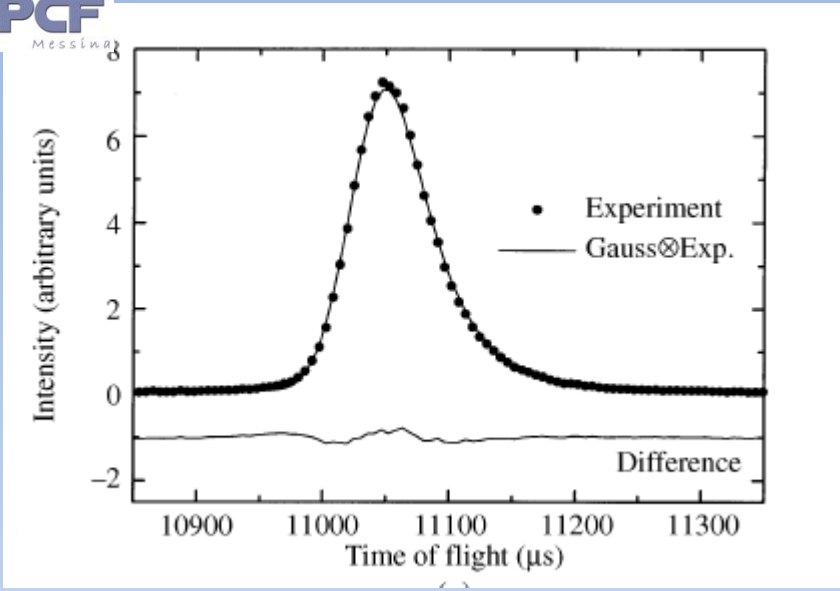

Experimental *110* Bragg diffraction peak in ***iron powder*** and least squares fit using the convolution of an exponential with a Gaussian function.

Santisteban et al. *J. Appl. Cryst.* **34**, 289-297(2001)

A large fraction of neutrons remain unused as usually only a small solid angle is covered with detectors but the neutrons are scattered over 4π.

In ***transmission***, the total neutron cross section of polycrystalline materials shows sharp discontinuities as a result of coherent elastic scattering on the lattice planes.

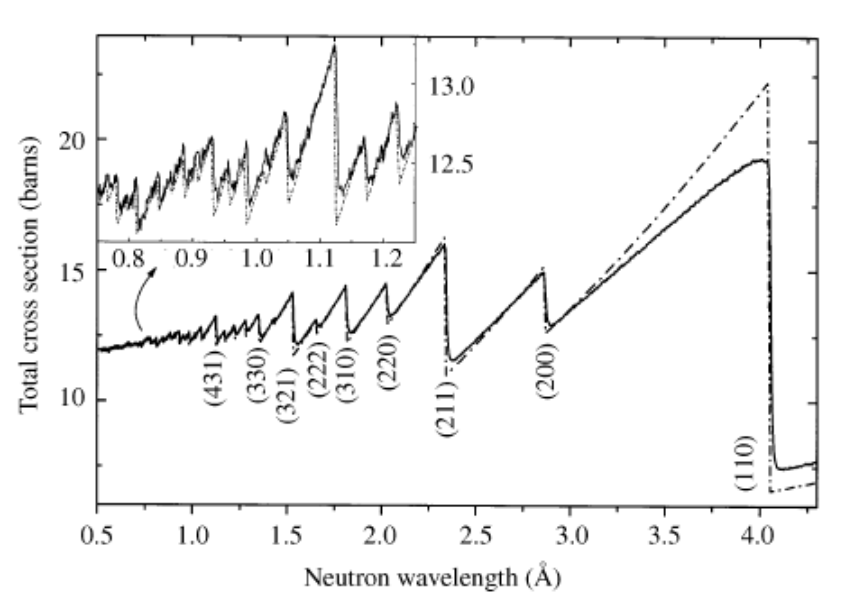

Total cross section of iron powder, displaying characteristic Bragg edges. Experimental values measured at ENGIN, ISIS (solid line).

Santisteban et al. *J. Appl. Cryst.* **34**, 289-297(2001)

These ***Bragg edges*** occur because, for a given hkl reflection, the Bragg angle increases as the wavelength increases until 2θ is equal to 180°. At wavelengths greater than this critical value, no scattering by this particular $\{hkl\}$ family can occur and there is thus an increase in transmitted intensity.

From Bragg's law, the wavelength at which this occurs is $\lambda = 2d_{hkl}$, giving a measure of the $\{hkl\}$ d-spacing in the direction of the incoming beam.

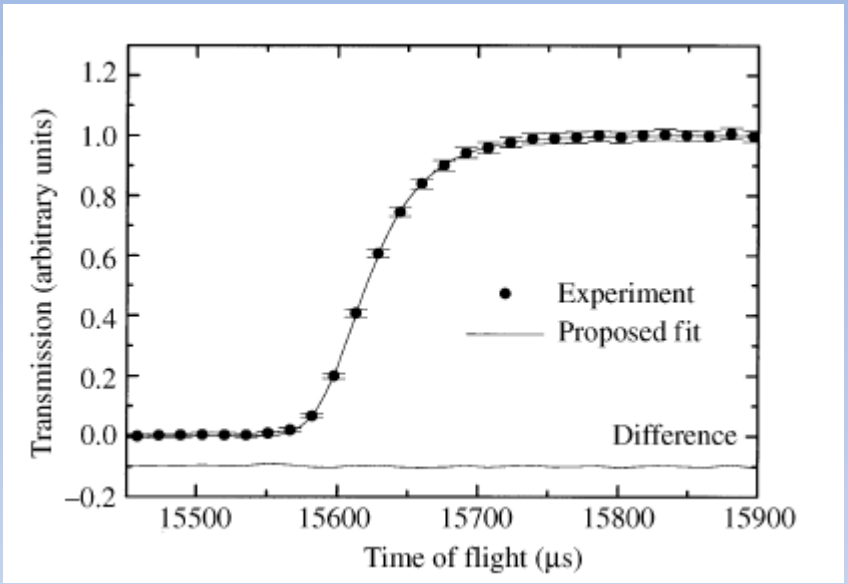

Experimental 110 edge in iron ***powder***. Spectrum acquired at ISIS on the ENGIN instrument

Santisteban et al. *J. Appl. Cryst.* **34**, 289-297(2001)

By acquiring transmission images in a well determined time relationship with the spallation pulse, we obtain a selection of neutron energies that will contribute to the image formation.

Different materials may have similar absorbing values when integrated over the full energy range of the neutron beam.
The following image depicts a composite cylinder where the outer part is made of iron and the inner part is copper.

The two parts are almost impossible to differentiate.

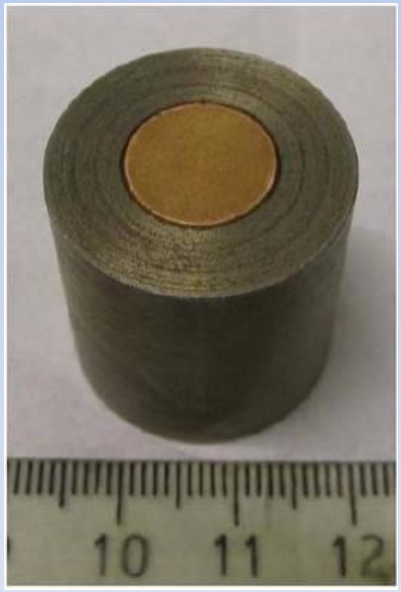

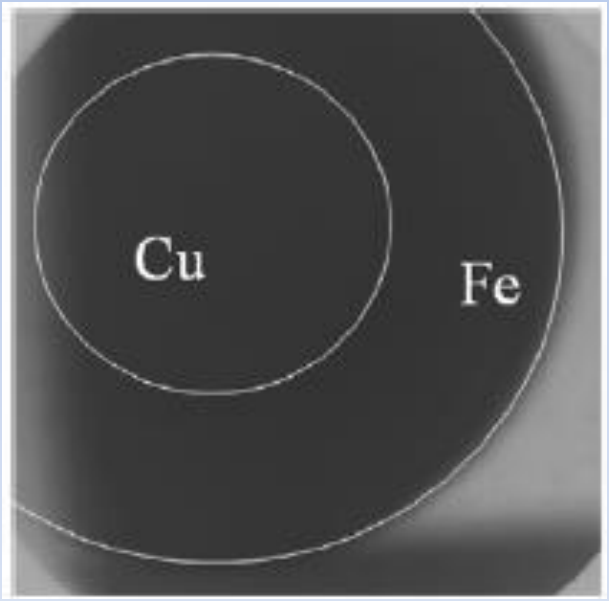

W. Kockelmann et al. Nuclear Instruments and Methods in Physics Research A 578 (2007)

Looking at the transmission spectra of the two materials it is possible to find energy values in which the transmission values are very different (because of the Bragg edges).

If we can take two pictures around that energy values, we can emphasize one or the other material.

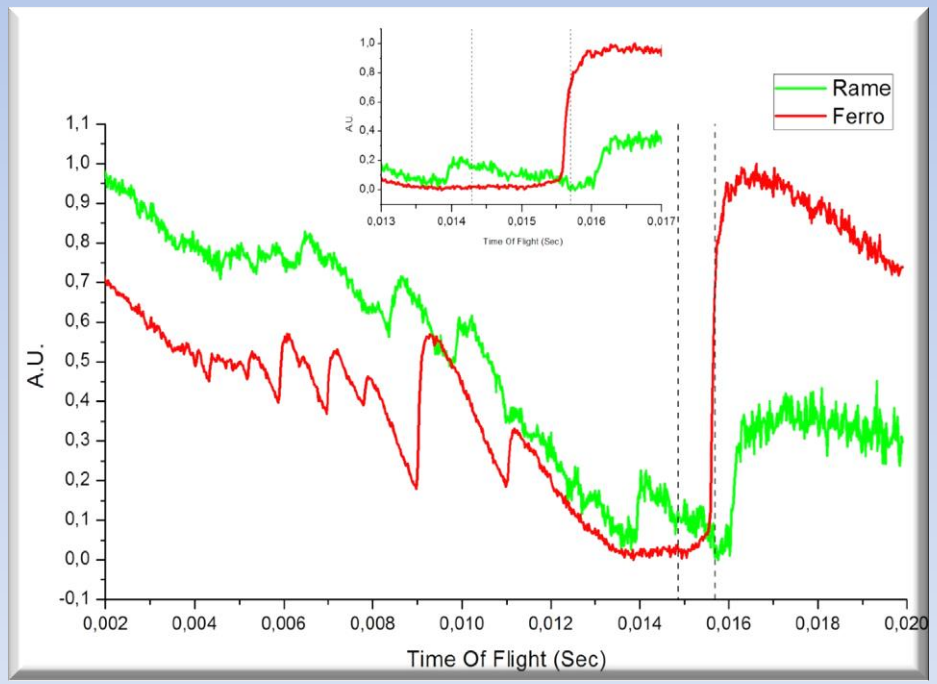

V. Finocchiaro - Tesi di Laurea specialistica - Università di Messina (2010)

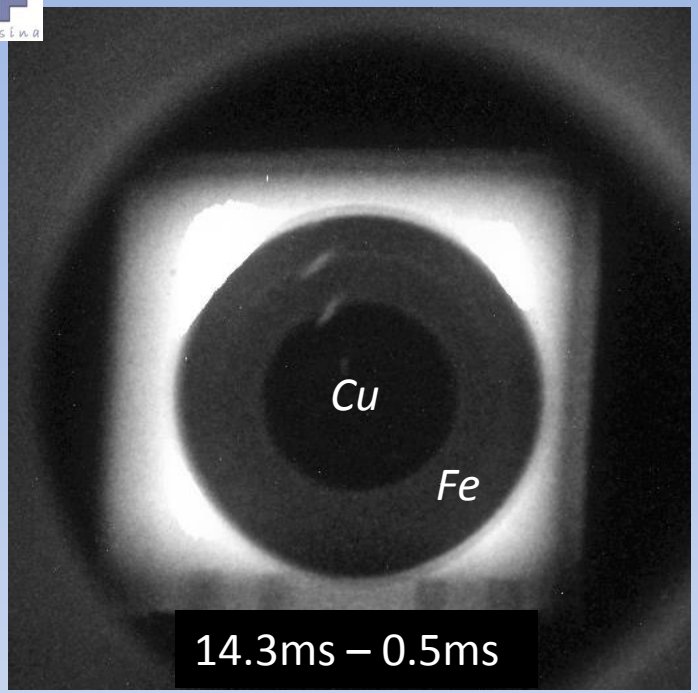

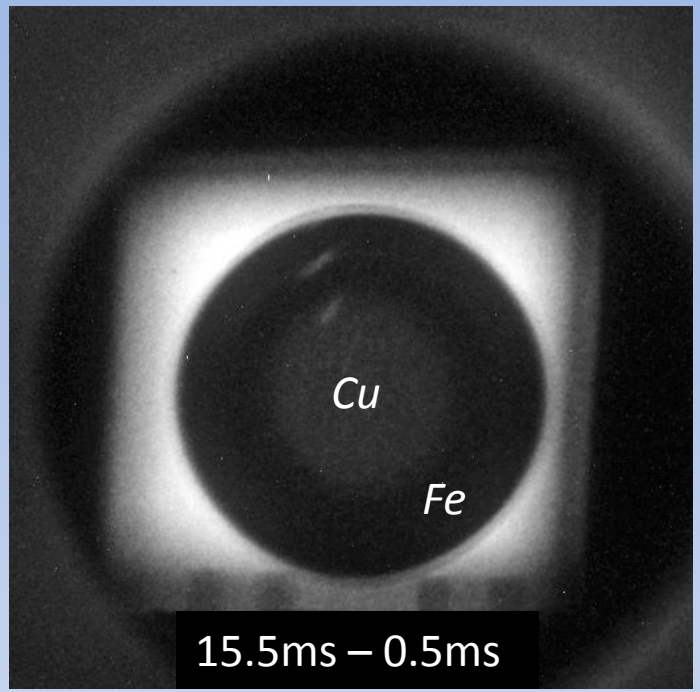

These images were acquired at the shown TOFs with multiple exposures of ***500µs*** and summing many partial images for a ***total exposure time of 8s*** (***400s of beam time*** @40Hz).

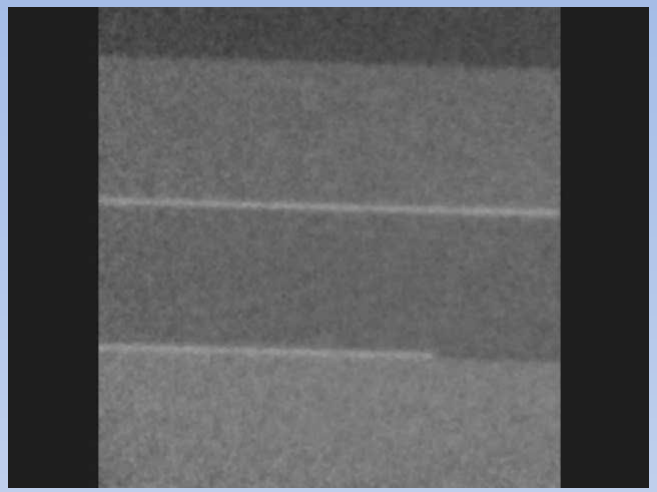

In this movie three different *Cu* crystals are imaged at different wavelengths in the range 1.8-4.3Å.

Each image is a sum of many images, each with an exposure time of ***25µs***, for a ***total exposure of 0.48s*** (**480s of beam time** @40Hz). The movie shows that the crystals are not very homogeneous.

This is one of a set of images of a ***Cu*** powder sample. The images were taken with ***TOF***s in ***7.0-9.4ms*** range. Each image is a sum of many images with an exposure time of ***25µs*** for a total exposure time of ***0.6s*** (***600s of beam time*** @40Hz).

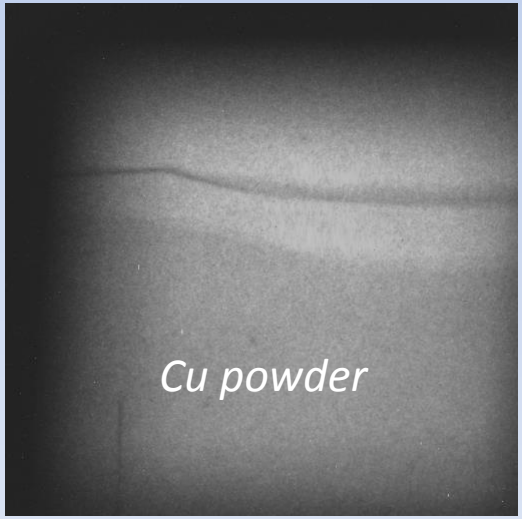

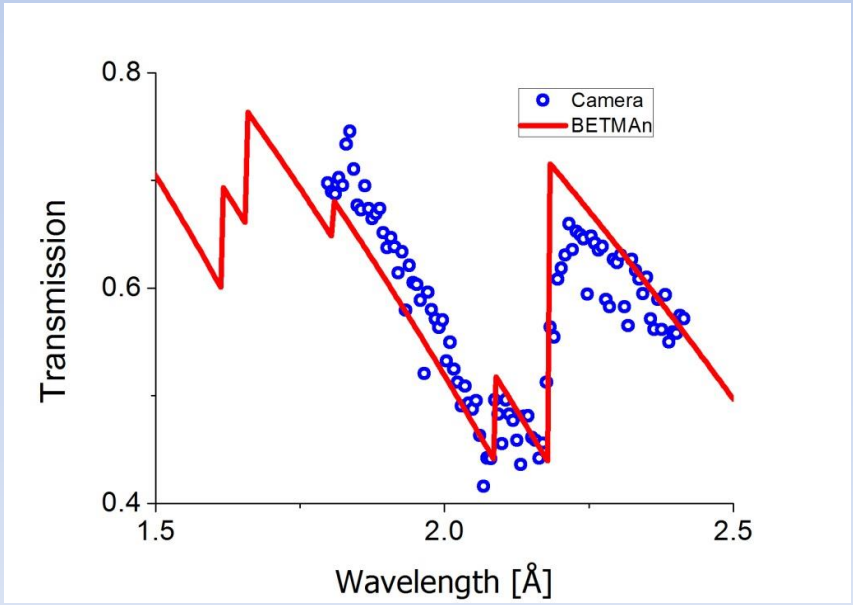

It is possible to select a portion of the images and to obtain a measure of the energy position and intensity of the Bragg edges present in the transmission spectrum.

In theory, this information can be extracted for each pixel which is present in the image so as to have a spatial distribution of the d-spacings.

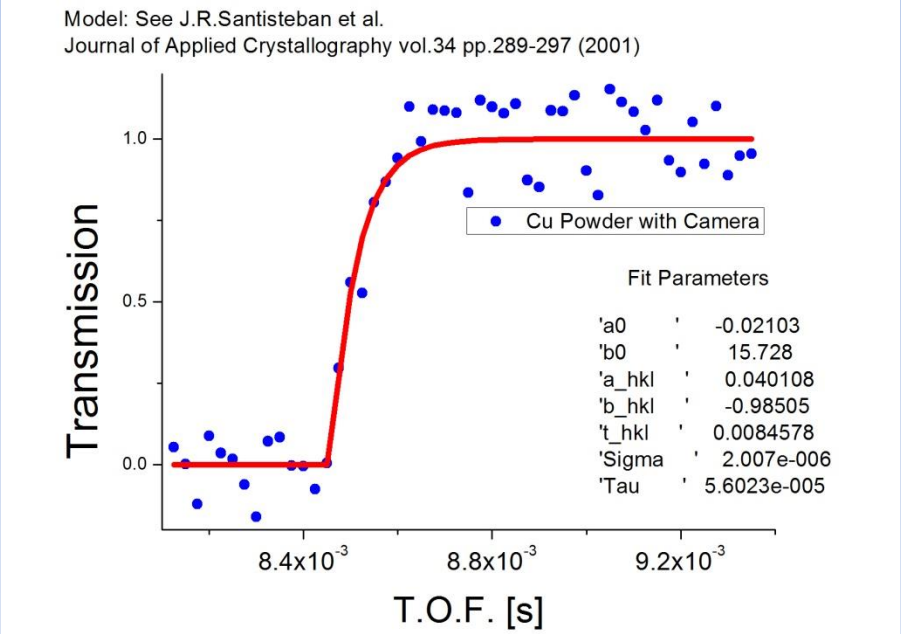

In the real world, the beam intensity available at present neutron facility is too low to give good signal to noise ratios for single pixel.

It is necessary to group many adjacent pixels to average their values and obtain reasonable signal to noise ratios.

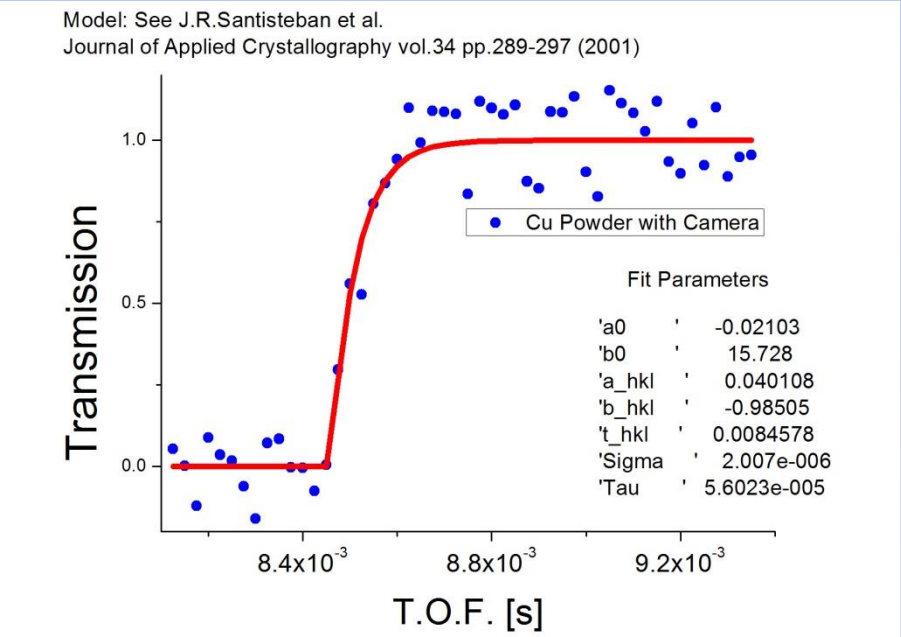

***How** TOF Neutron Imaging is done ?*

<u>There are not, at present, imaging systems that fulfill all the requests from scientists</u>.

The requests are:

- ***Time resolution*** in the range of ***10µs***
- ***Spatial resolution*** in the range of ***100µm***
- ***Reasonable acquisition times*** (from seconds to tens of seconds)
- ***Good signal to noise ratios***
- ***Wide Field-of-View (>20x20cm^2)***

CCD CAMERA based image sensors

***C**harged **C**oupled **D**evices* (**CCD**) are image sensors developed to be used mainly in consumer cameras.

CCD**s are **very linear devices: the number of collected electrons in a pixel is proportional to the number of incident photons.

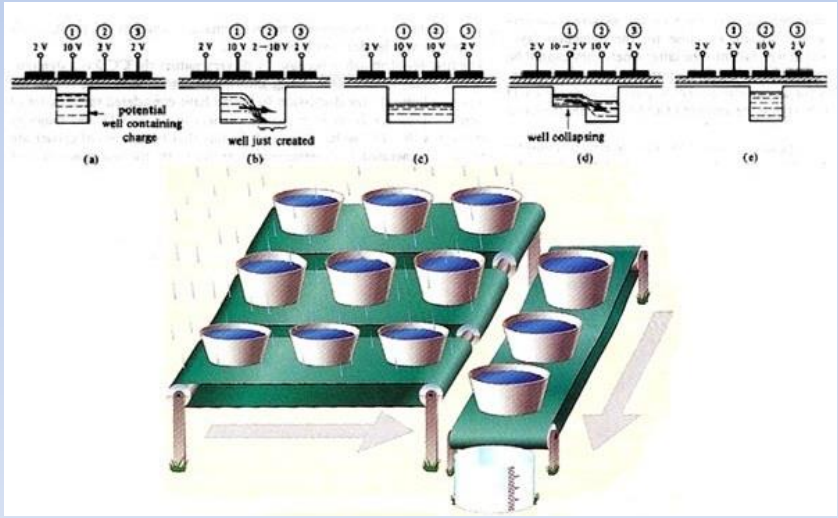

http://www.science.ca/images/scientists/s-boyle-infographic.jpg

CCDs have a large number of pixels allowing a good spatial resolution.

As an example, a ***CCD*** sensor with 1000x1000 pixels can imagine a field of view of 10x10cm^2 with a ***spatial resolution*** of ***100µm***.

The intrinsic ***noise*** of ***CCD***s is low and can be reduced by ***cooling*** the sensor. Since the main contribution is the ***readout noise,*** it can be lowered by slowing the readout process

The requested ***time resolution*** can be obtained by interposing between the lens and the ***CCD*** sensor a ***<u>Gated</u> Image Intensifier.***

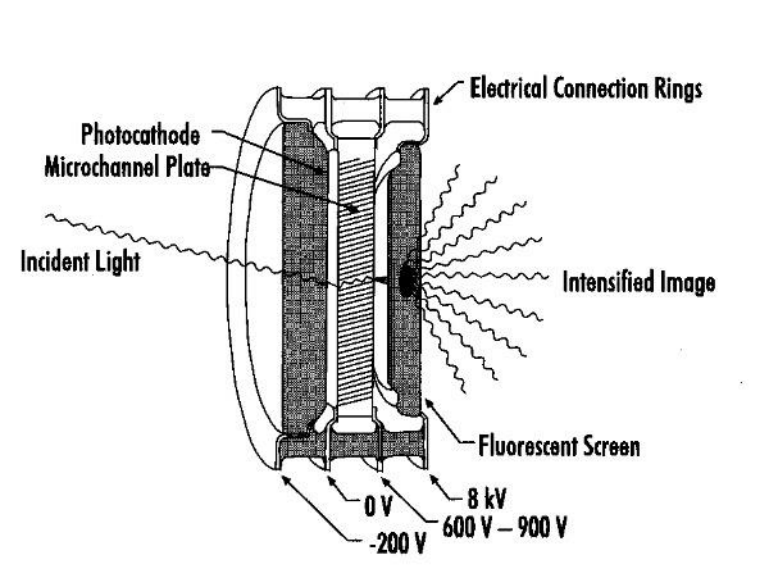

The photons reaching the microchannel plate generate charged particles that are accelerated by an electric field and made to collide with a fluorescent screen.

The micro channel plate is a thin disk (<1 mm thick) of honeycombed glass, and each of the honeycomb channels (~6-10μm) has a resistive coating.

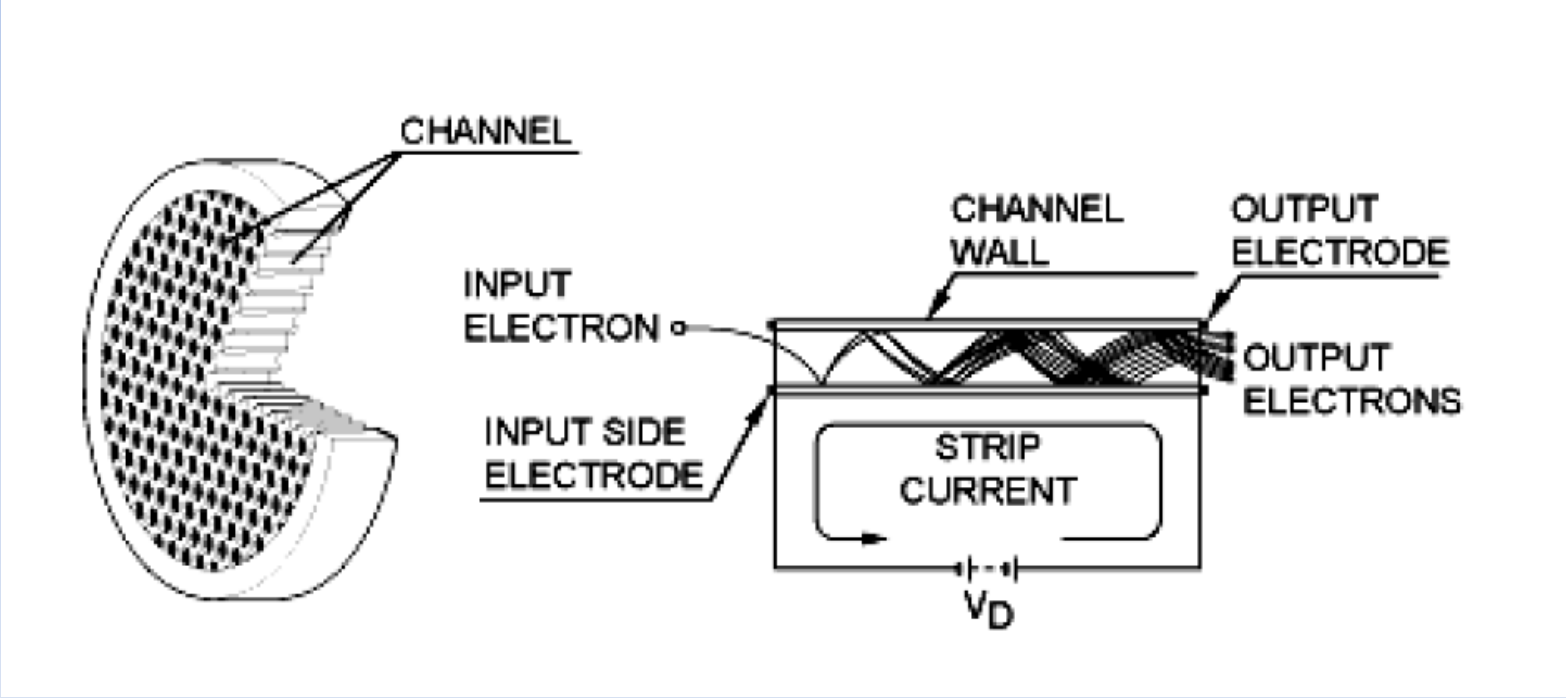

The micro channel plate has a high potential across it (500 to 1000 V) so that the photoelectron will cascade down the channel producing secondary electrons; the resultant amplification can be up to 10^4.

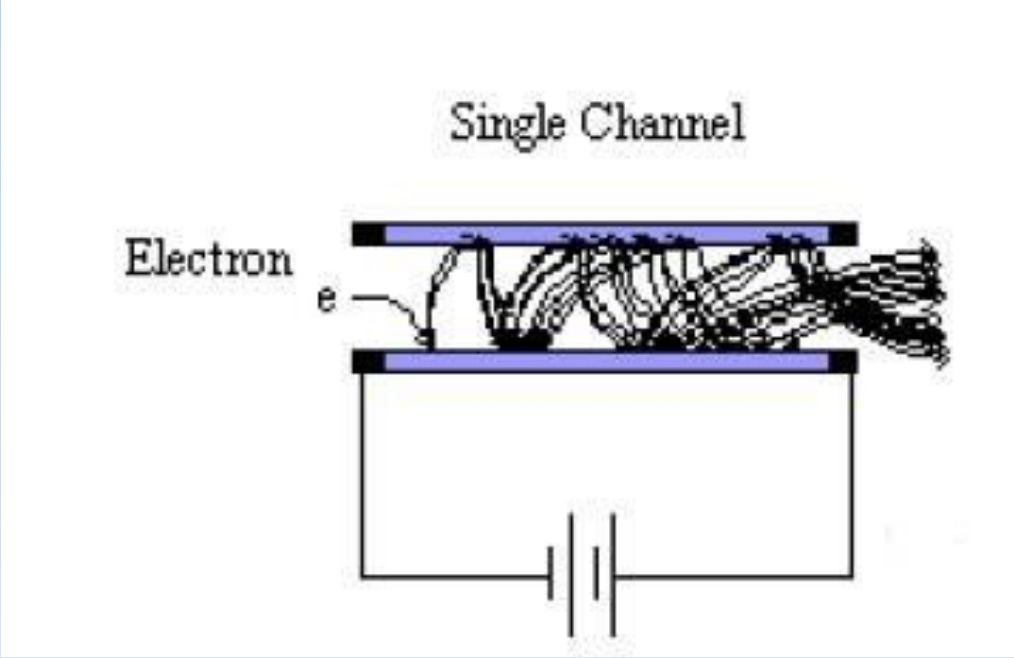

The main amplification of an image intensifier is due to the electron cascade in the channel plate. ***Varying the voltage across the channel plate will control the gain***.

Changing the ***voltage across the microchannel plate it is possible to completely stop the light*** that reach the CCD sensor.

In this way ***you may control the exposure time by applying voltage pulses across the microchannel plate.***

Gate time <5ns can be obtained so ***the requested time resolution (>10μs) can be easily obtained.***

Typically ***the on/off ratio of the intensifier is 1:10^8*** in the visible region.

Since the intrinsic noise of the ***CCD*** can be made very low by cooling the sensor, ***it is possible to make very long exposures and turn on, repetitively, for short time periods the intensifier.***

The obtained image is a sum of many partial images without the need to transfer each single image outside the chip with the associated readout noise. This procedure is called ***"Integrate on Chip"***.

These two images were obtained with a total exposure time of ***600s***, and summing ***24000*** partial images with an exposure time of ***500µs*** each

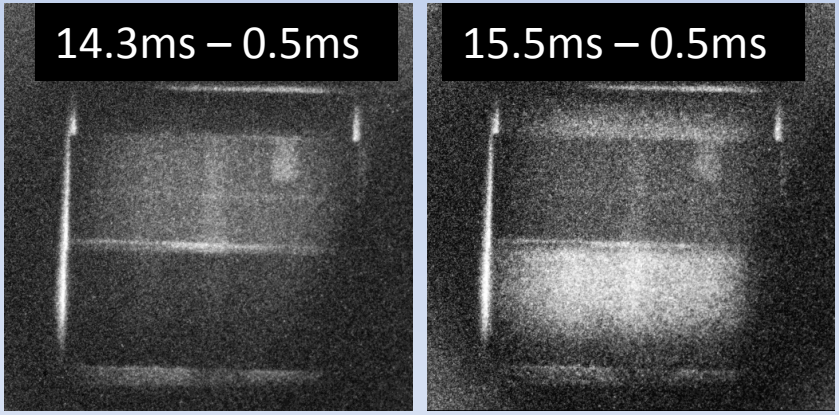

The image shows a schematic view of an ***Andor iStar*** camera with which we have acquired the TOF images.

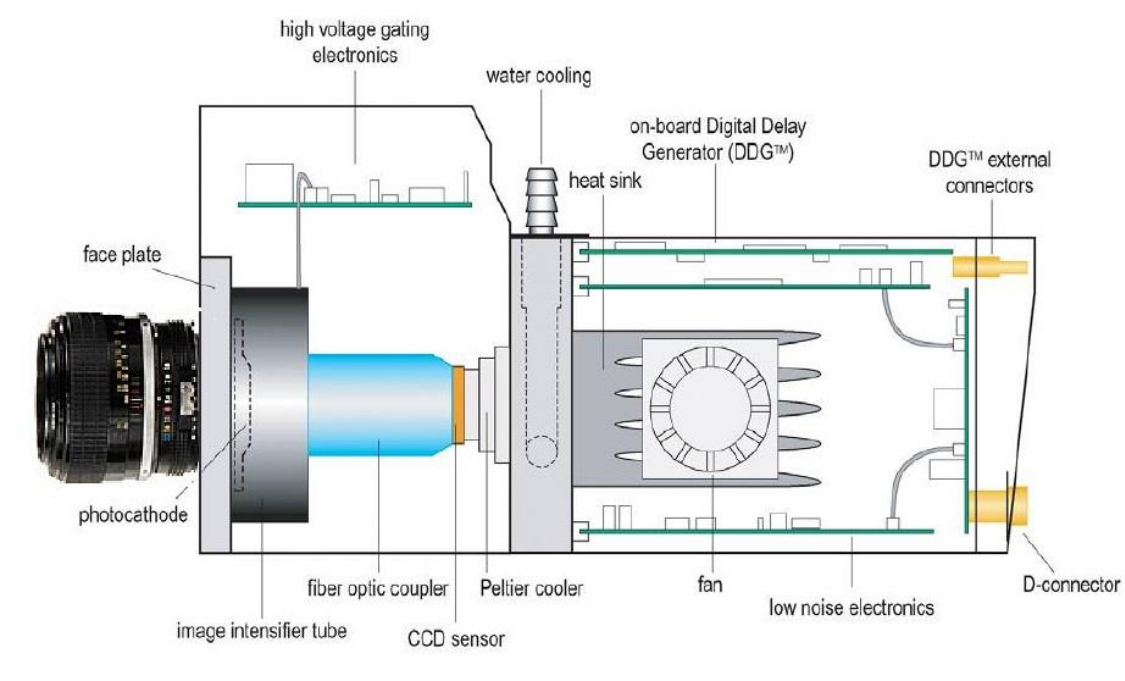

Very bright lenses are ***a must*** in order to reduce the required total exposure time.

While ***iCCD***s gate times are well below the requested time resolution (remember: >10μs) the common used scintillator screens (***^{6}LiF/ZnS*** based) have not equally satisfactory timing characteristics.

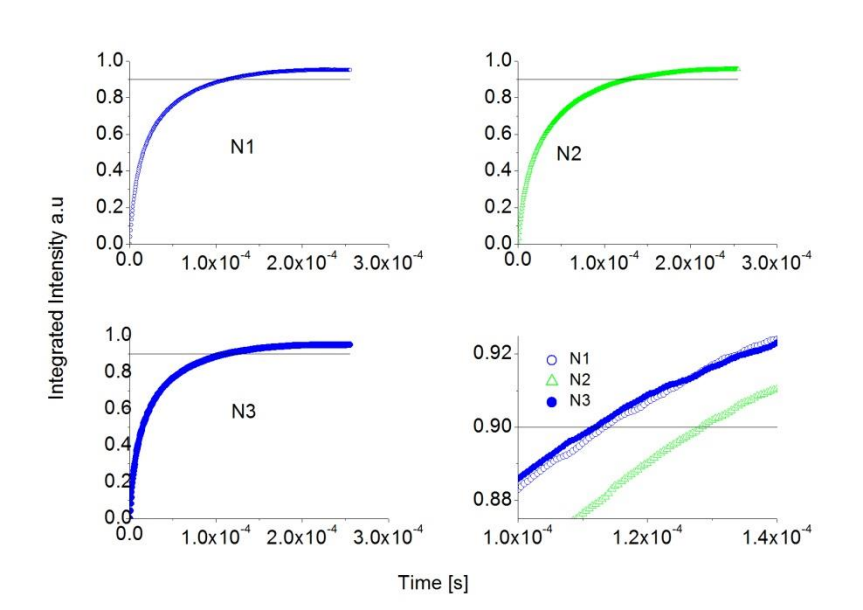

The intensity of the light produced by a neutron hitting the scintillator decays rather slowly.

G. Salvato et al. *Nucl. Instr. and Meth.* A **621** 489–492 (2010)

Some of the technical requirements for TOF imaging can be fulfilled by a CCD based system with ***two major drawbacks***.

- timing characteristics of the scintillators and
- ***the needed acquisition time***.

During the time interval (***~500s*** at ROTAX) needed to acquire an image, ***only a single wavelength*** can be explored.

A ***terrible waste*** of (very expensive) beam time.

At future facilities (IMAT as an example) the beam intensity can be an order of magnitude greater than that available at ROTAX and the acquisition time can be an order of magnitude lower (***~50s***).

While this will be a significant improvement, ***other new, more efficient, detectors are required***.

A new sensor that has been proposed as a more efficient, time resolved, image detector is derived from a solid-state sensor which has been originally developed for high energy particle detectors.

The sensor is based on ***neutron-to-charged particle*** conversion in ***^{10}B***-doped microchannel plates (***MCP***s)

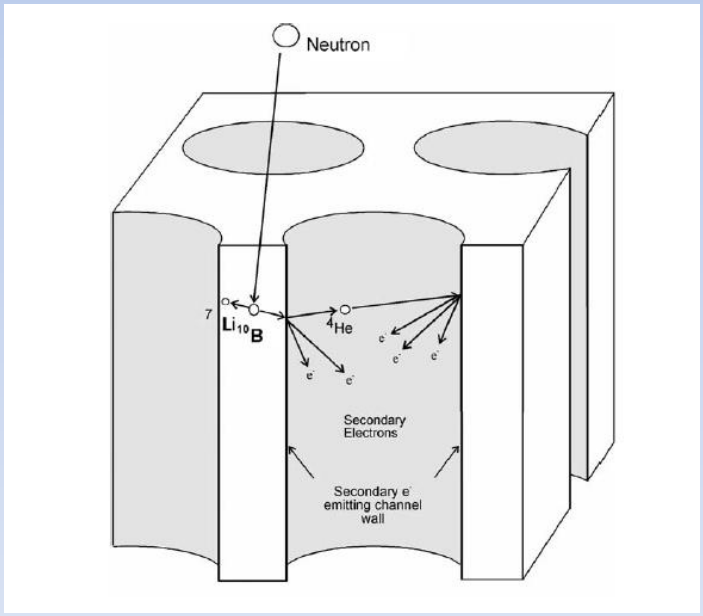

The neutron detection exploits the ^{10}B(n, α) ^{7}Li reaction.

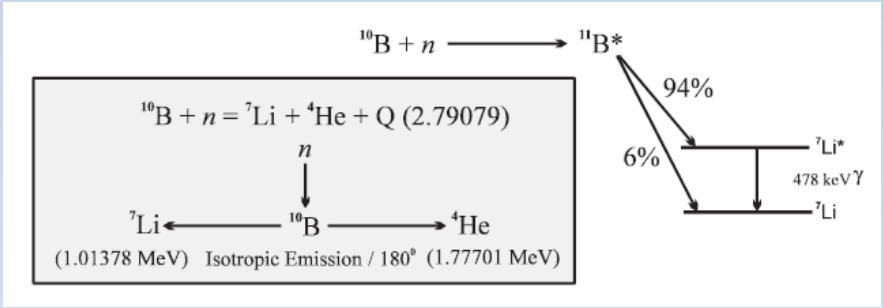

A.S. Tremsin et al. *Nucl. Instr. and Meth.* A **539** 278–311 (2005)

The ***alpha*** and ***^{7}Li*** charged particle reaction products emerge from the channel wall surfaces into an open channel.

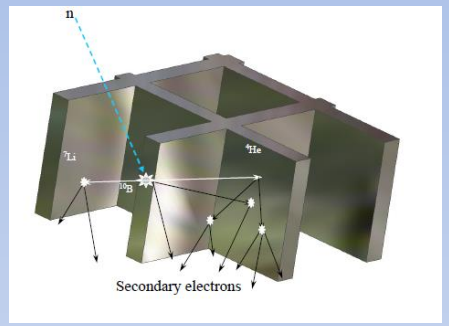

As these heavy particles cross the surface, a relatively large number of secondary electrons (and other species) are liberated to ***generate a strong electron avalanche*** and an output pulse.

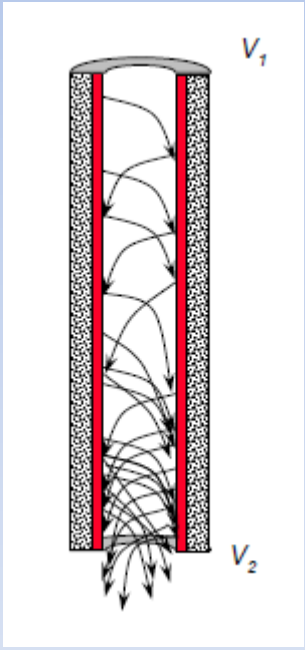

A.S. Tremsin et al. **IEEE NSS 2007, October 2007**

The detection characteristics of ^{10}***B***-doped ***MCP***s can be very effectively applied to neutron detection and imaging, with ***position sensitivity*** on the order of ***10µm*** and t***iming accuracy*** down to ***100ps***.[1]

For high counting rate applications, the neutron sensing ***MCP***s are combined with a fast readout device: ***Timepix/Medipix2***.

Medipix2 is realized in CMOS technology and has a spatial resolution of ***~55µm***.

[1] A.S. Tremsin et al. *Nucl. Instr. and Meth.* A **539** 278–311 (2005)

The present ***Medipix2*** based readout has ***256x256*** pixels with an active area of ***14x14mm²***

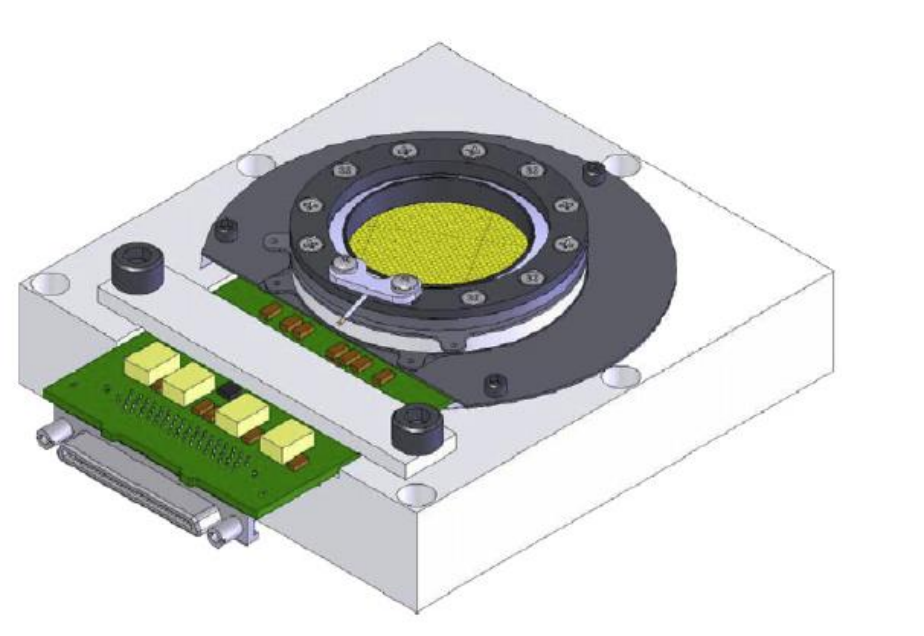

A.S. Tremsin et al. *Nucl. Instr. and Meth. A* **592** 374–384 (2008)

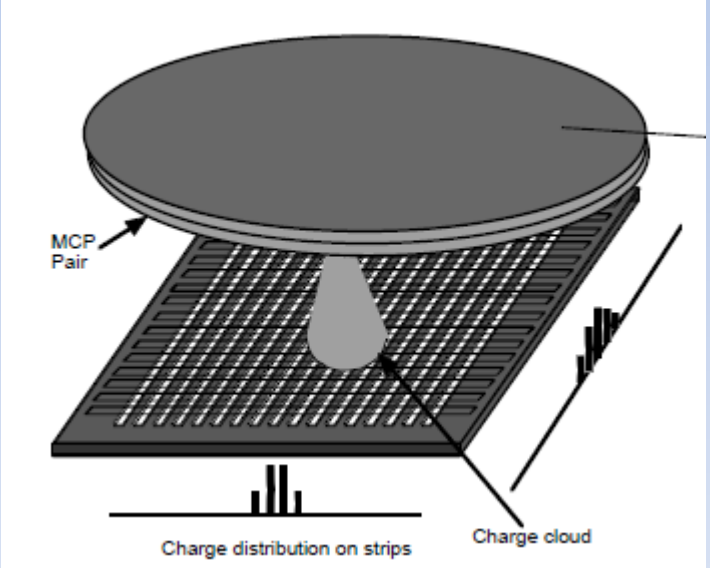

A.S. Tremsin et al. **IEEE NSS 2007, October 2007**

Energy-resolved radiography with the ***MCP*** detector on ENGIN-X.
Time width: ***100µs***.

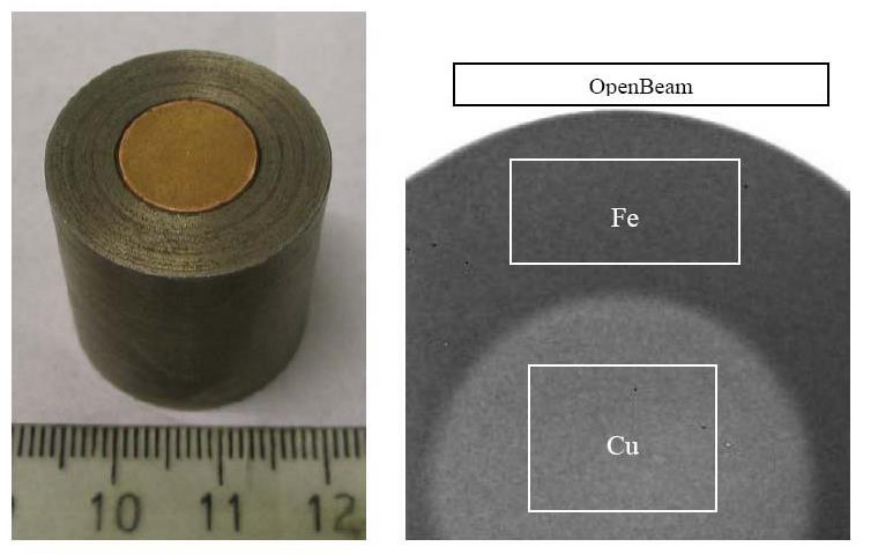

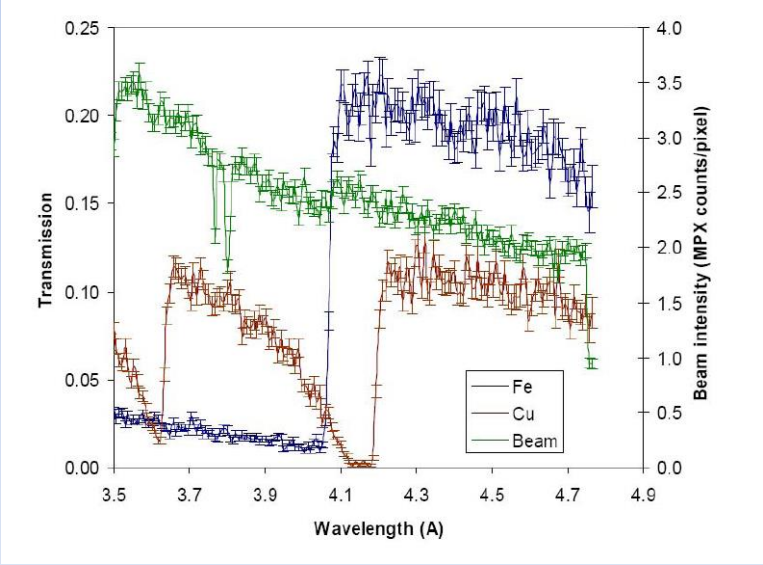

Bragg edge spectra of the two metals compared to the open beam spectrum.

A.S. Tremsin *Report on neutron transmission measurements at ISIS with a high resolution MCP detector* (2008)

The detector is still ***in the experimental phase.*** Some high-resolution images were obtained at a ***low counting rate*** (on the order of ***1kHz***) limited by the currently implemented ***serial readout electronics***. In the present setup the ***Timepix*** frame can be read out in ***33ms***, while the frame shutter duration can be as small as 10µs.[1]

Essential improvements are necessary for both obtaining a ***bigger Field of View*** and ***speeding-up the readout process***. The ***Radiation Hardness*** of the readout chip must be checked too.

[1] A.S. Tremsin et al. *Nucl. Instr. and Meth. A* **592** 374–384 (2008)

Recently, ***a new family of position sensitive detectors*** has emerged. Such devices are based on ***Wavelength Shifting (WLS) Fibers*** and ***Position Sensitive Photomultipliers***.

Two schematic views of the detector are shown: a) from the side, b) from the top.

The Fiber-optics taper optically couple the scintillator with the WLS fibers and provide a small (3x) image magnification.

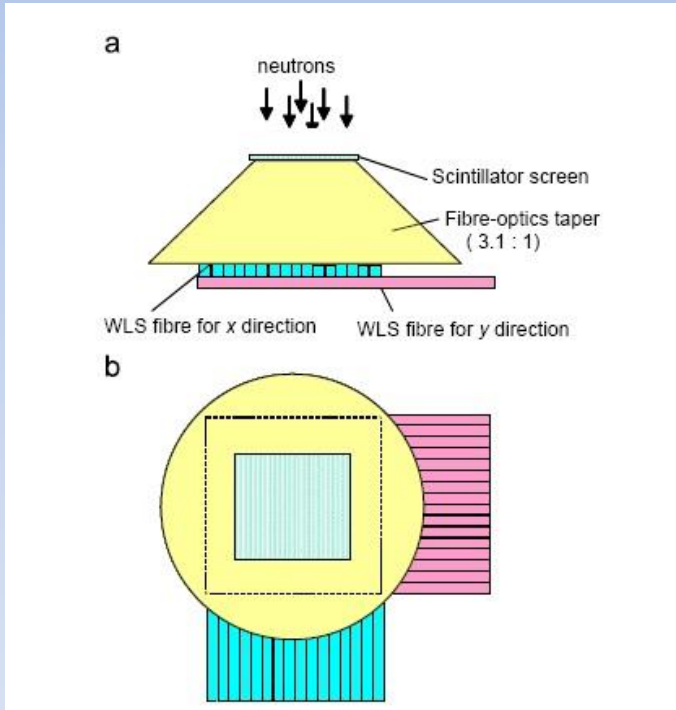

T. Nakamura et al. *Nucl. Instr. and Meth. A* **604** 158–160 (2009)

The ***WLS fibers*** absorb photons in a certain band and emit photons in a different one.

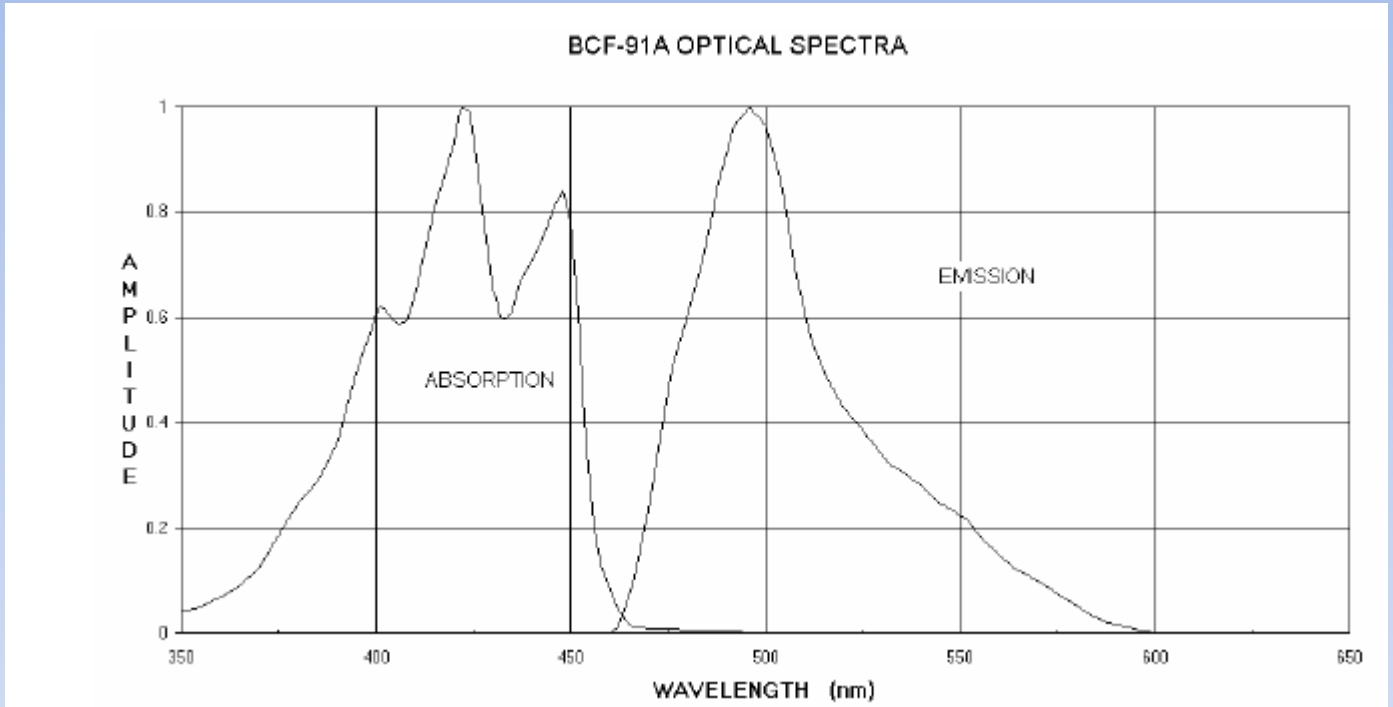

The absorption band maximum is centered about at the emission peak of the $^{6}LiF/ZnS(Ag)$ scintillator.

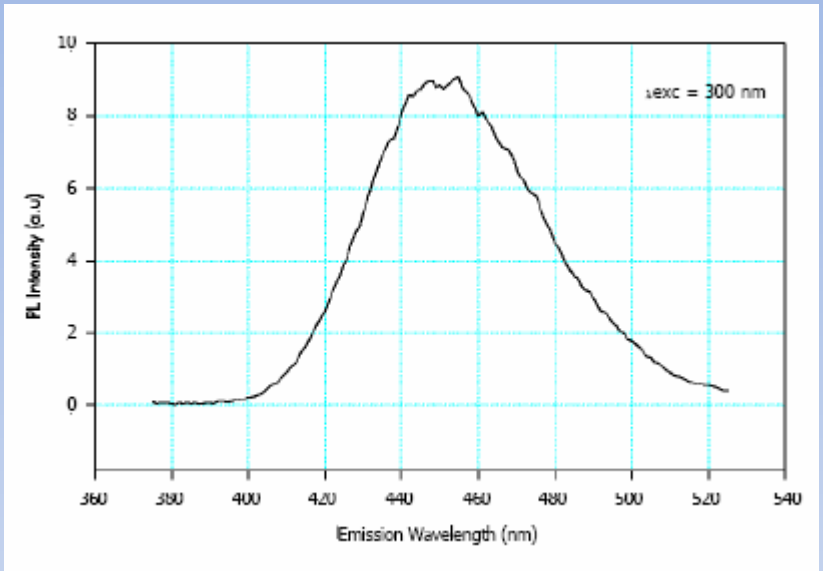

The neutrons impinging on the $^{6}LiF/ZnS(Ag)$ scintillator screen produce photons (~160000) in the blue region peaked at ~450nm (see figure).

Some of the photons, that enter a WLS fiber from the side, are adsorbed and produce photons, with different wavelengths, that travel towards the fiber ends. Some other photons exit the fiber at the opposite side and enter the perpendicular ones.

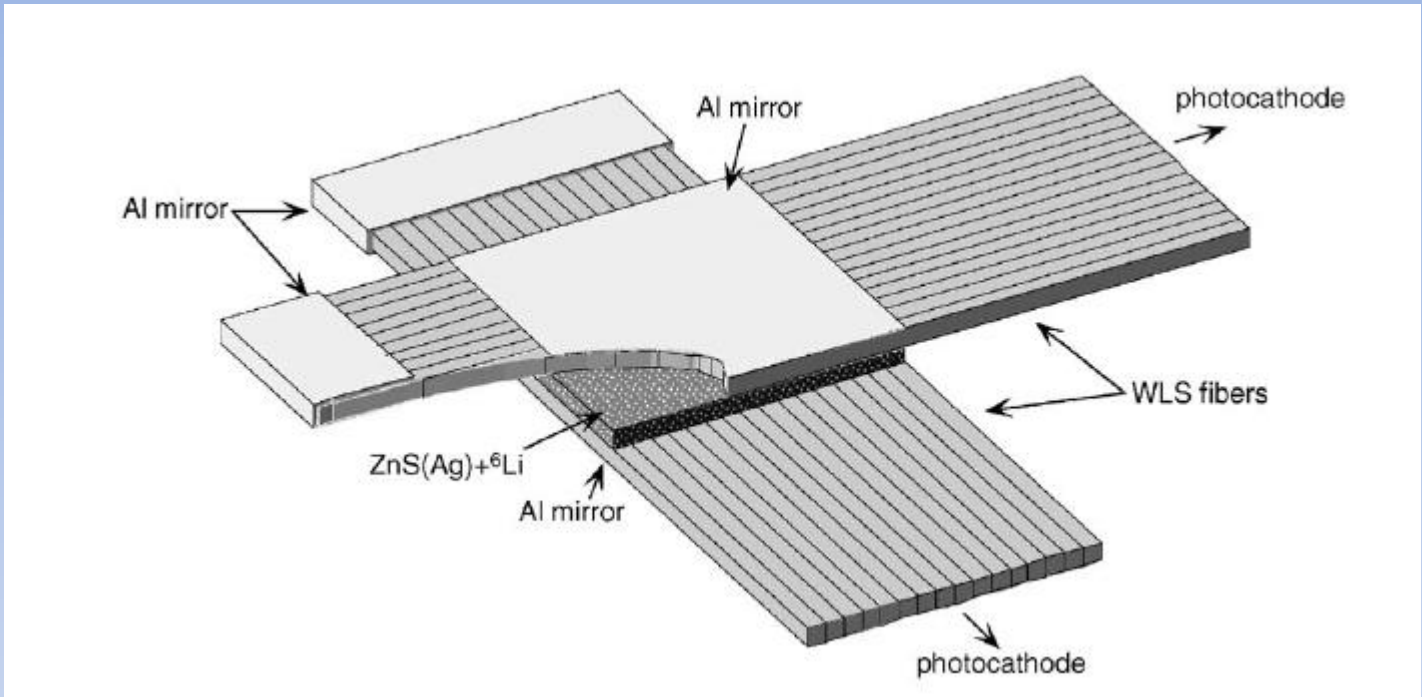

Here a variant of the device is shown: it has no spatial magnification and ***Al*** mirrors to increase the light intensity reaching the fiber end.

A. Gorin et al. *Nucl. Instr. and Meth. A* **479** 456–460 (2002)

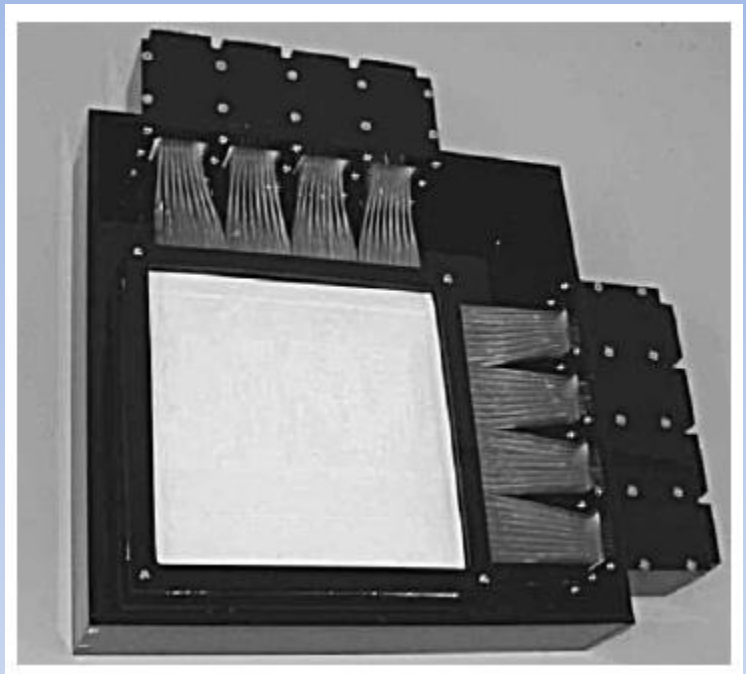

Here a real device is shown: it has a ***128 x128mm²*** sensitive area and a ***500x500µm²*** pixel size.

K. Sakai et al. *Nucl. Instr. and Meth.* A **529** 301–306 (2004)

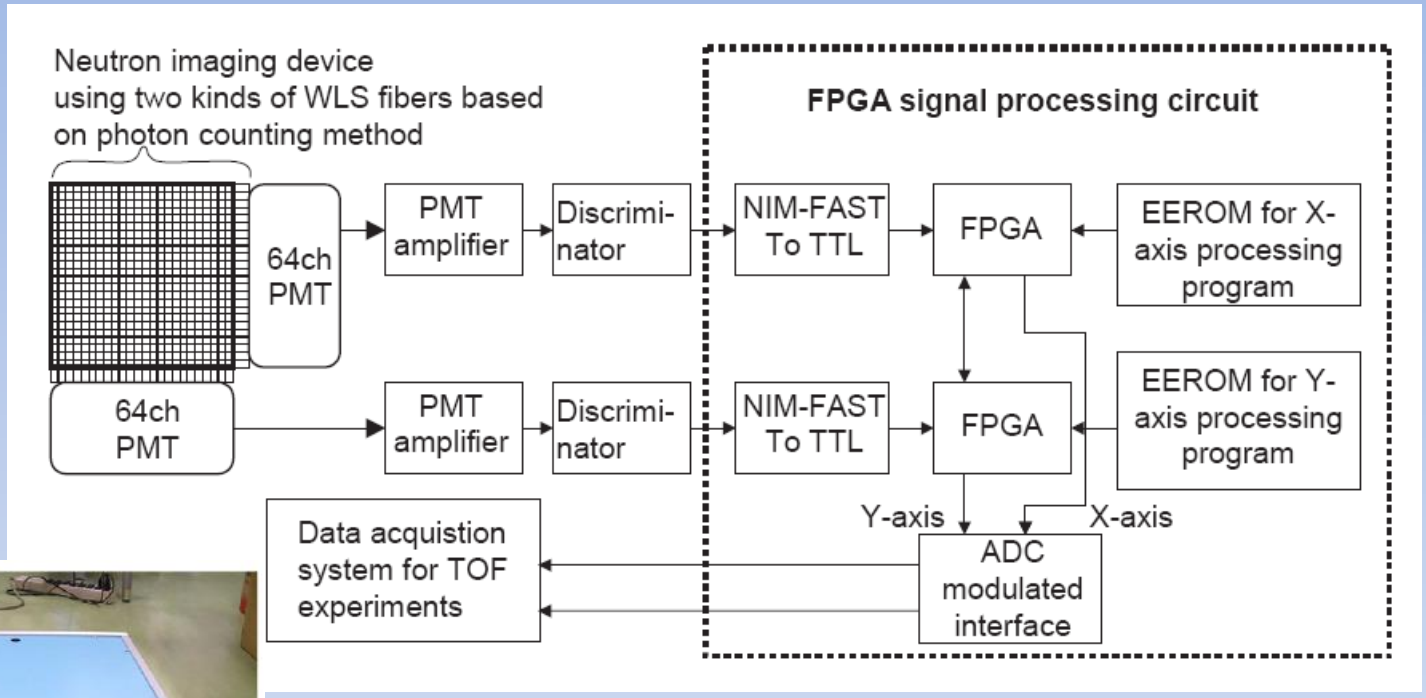

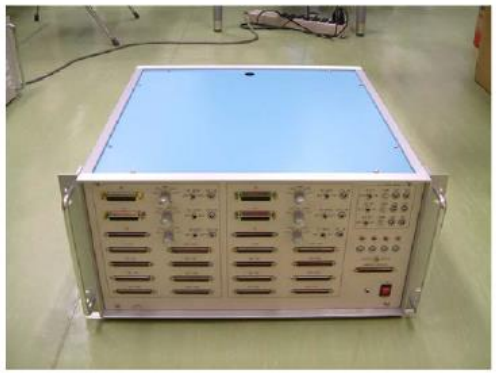

Readout schematics and a *256x256* pixel signal processing module.

M Katagiri *Nucl. Instr. and Meth.* A **529** 254–259 (2004)

Neutron detection efficiency of a WLS based detector with a single or a double scintillator sheet

M. Katagiri et al. *Nucl. Instr. and Meth.* A **573** 149–152 (2007)

Table 2
Neutron detection efficiencies for thermal neutrons

Upper ZnS/^{6}LiF	^{6}LiF:15 mg/cm^2	29.5%
Lower ZnS/^{6}LiF	^{6}LiF:23 mg/cm^2	36.4%
Both ZnS/^{6}LiF	Total:38 mg/cm^2	55.8%